ASSESSMENT OF THE EFFECTS OF SUPEROXIDE-GENERATING AGENTS ON THE GROWTH AND VIABILITY OF *ESCHERICHIA COLI* USING TRADITIONAL MICROBIOLOGICAL METHODS AND FLUORESCENCE METHODS

A thesis presented to the faculty of the Graduate School of
Western Carolina University in partial fulfillment of the
requirements for the degree of Master of Science in Biology.

By

Jennifer Lynn Patterson

Director: Dr. Lori B. Seischab
Assistant Professor of Biology
Biology Department

Committee Members: Dr. Christopher T. Coburn, Biology
Dr. Jack S. Summers, Chemistry and Physics

July 2010

ACKNOWLEDGEMENTS

I would like to thank Dr. Lori Seischab for allowing me to work on this project and for her advice and guidance during challenges encountered during completion of this research. I would also like to thank Drs. Jack Summers and Chris Coburn for serving on my thesis committee, Dr. Sabine Rundle for her advice and help, and Dr. Seán O'Connell for serving as my thesis reader.

I would also like to thank my family; without their love and support I would not have continued on with my education.

TABLE OF CONTENTS

LIST OF TABLES

LIST OF FIGURES

LIST OF EQUATIONS

ABSTRACT

ASSESSMENT OF THE EFFECTS OF SUPEROXIDE-GENERATING AGENTS ON THE GROWTH AND VIABILITY OF *ESCHERICHIA COLI* USING TRADITIONAL MICROBIOLOGICAL METHODS AND FLUORESCENCE METHODS

Jennifer Lynn Patterson, M.S.

Western Carolina University, July 2010

Director: Dr. Lori B. Seischab

The effects of superoxide-generating agents on the growth and viability of *Escherichia coli* was investigated using two different strains, a lab strain (ER2566) and a clinical isolate (ATCC 4157). Endogenous superoxide was generated using the redox-cycling agent paraquat, while exogenous superoxide was generated using the xanthine/xanthine oxidase (X/XO) enzyme system. Using optical density measurements to monitor culture growth, the bacteriostatic effect of paraquat was tested in three different growth media: Luria-Bertani broth, double strength Luria-Bertani broth, and nutrient broth. For both strains, paraquat toxicity was greatest in nutrient broth, with toxicity in each medium dependent upon the time of paraquat addition following inoculation. Protection against paraquat toxicity by salts and yeast extract was suggested by the differences observed between growth rates of ER2566 treated cultures in each medium. Addition of the copper/zinc superoxide dismutase inhibitor diethyldithiocarbamate decreased paraquat toxicity, consistent with its role in induction of the superoxide response regulon (soxRS). Based on colony-forming unit (CFU) counts, the toxicity of X/XO-generated superoxide on ER2566 was found to be altered by pH, with cell viability lower at a pH of 6.5 than at 7.5. Using CFU counts obtained with

the spread-plate method and total cell counts obtained with a hemacytometer, the relationship between optical density and cell number was found to be different between cultures of the two strains at both log and stationary phases. Reliable cell counts were necessary to avoid the inner filter effect otherwise encountered during optimization of the BacLight Bacterial Viability Kit for ATCC 4157. Assessment of cell viability following X/XO treatment with the BacLight kit indicated this method was more sensitive than the traditional spread plate method for determining cell viability.

INTRODUCTION

1. EFFECTS OF OXIDATIVE STRESS ON THE BACTERIAL CELL

Reactive oxygen species (ROS) including superoxide, hydrogen peroxide, and hydroxyl radicals are present within all aerobic cells. On its own, superoxide has many deleterious effects within the cell, one of which is the oxidation of iron sulfur clusters [4Fe-4S] that serve as cofactors in a family of enzymes known as dehydratases. This family includes the enzymes aconitase, dihydroxy acid dehydratase, 6-phosphogluconate dehydratase, fumarase A, and fumarase B (Fridovich 1995). These clusters are composed of four iron atoms connected by inorganic sulfide, three of which are coordinated to sulfur atoms of cysteine residues, with the fourth iron coordinated to water and exposed to solvent (Figure 1). As a result of oxidation by superoxide, this fourth iron is removed and the enzyme is deactivated.

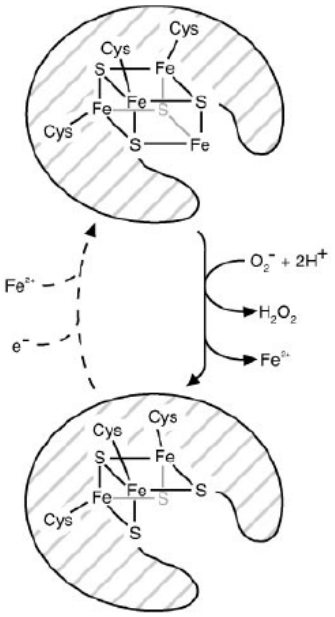

Figure 1. Superoxide oxidation of the iron-sulfur cluster of a dehydratase (Imlay 2003).

Iron-sulfur clusters were essential to formation of primordial enzymes as both iron and sulfur were abundant in Earth's early anaerobic atmosphere (Imlay 2006). However, oxygenation of the atmosphere forced microorganisms unable to find alternate electron transfer pathways to remain obligate to anaerobic environments. The inactivation of these enzymes halts biosynthesis of amino acids and progression of the TCA cycle (Korshunov and Imlay 2002).

In addition to inactivating enzymes with iron-sulfur clusters, superoxide serves as a precursor to the formation of additional reactive oxygen species including hydrogen peroxide and the hydroxyl radical. Hydrogen peroxide can be converted to harmless molecules, water and oxygen, by the enzyme catalase. However, it can also react with iron released from damaged iron-sulfur clusters to produce hydroxyl radicals, a reaction known as the Fenton reaction (Equation 1).

$$H_2O_2 + Fe^{2+} \rightarrow OH^- + FeO^{2+} + H^+ \rightarrow Fe^{3+} + OH^- + HO\cdot \quad (1)$$

While both superoxide and hydrogen peroxide are limited in their reactivity, the neutral hydroxyl radical is highly reactive and nonselective, making it extremely detrimental to the cell due to its ability to damage DNA, proteins, and membranes. The ability of organisms to adapt to oxygen is most extreme in bacteria. Bacteria exhibit a wide range of oxygen tolerance, with the two extremes being obligate anaerobes and obligate aerobes. In addition, microaerophiles require environments where the oxygen concentration is less than 20% and aerotolerant bacteria are unaffected by changes in oxygen concentration.

2. CYTOSOLIC SUPEROXIDE PRODUCTION IN BACTERIA

Reactive oxygen species are not intentionally produced by the cell but occur as an unavoidable consequence of aerobic respiration. Molecular oxygen is an ideal molecule to serve as the terminal electron acceptor in aerobic respiration as a large amount of energy is released once its double bond is broken. In addition, it does not easily react with other biomolecules minimizing damage to amino acids and nucleic acids. This limited reactivity is due to its triplet state. The two unpaired spin-aligned electrons present in its pi antibonding orbital restrict electron exchange with most molecules. Therefore, only molecules capable of univalent electron transfer are able to transfer electrons to molecular oxygen (Imlay 2003). Redox enzymes of the respiratory chain are capable of autooxidation through the electron transfer capability of their flavin cofactors, and collision of oxygen with reduced flavins results in the reduction of diradical oxygen to the free radical superoxide. Several enzymes with this ability have been identified in *Escherichia coli* including NADH dehydrogenase II, succinate dehydrogenase, sulfite reductase, and fumerate reductase (Messner and Imlay 2002). The amount of superoxide produced as a byproduct of aerobic respiration within the cytosol of *E. coli* is estimated to be 5 μM per second (Imlay 2003). Once produced, superoxide remains within the cytoplasm of the cell as its negative charge prevents its passive diffusion through the plasma membrane.

3. INTRACELLULAR SUPEROXIDE PRODUCTION IN BACTERIA BY EXTERNAL AGENTS

The ability of bactericidal antibiotics to kill bacteria was long attributed solely to their capacity to inhibit the synthesis of critical cell macromolecules such as DNA, proteins, and the cell wall (Kohanski et al. 2007). However, for each of the three major classes of bactericidal antibiotics, aminoglycosides, quinolones, and β-lactams, it is now known that part of their lethality is due to the production of superoxide. Each antibiotic causes an increase in the consumption of NADH by increasing the production of NADH dehydrogenase I which results in hyperactivation of the electron transport chain, thereby increasing the amount of superoxide produced. As described above, as a result of damage caused by superoxide, highly reactive hydroxyl radicals are generated through the Fenton reaction. Hydroxyl radical formation is key to the lethality of bactericidal drugs. Bacteriostatic drugs that slow bacterial growth do not promote generation of hydroxyl radicals (Kohanski et al. 2007).

A well-known external agent used for the generation of intracellular superoxide is the herbicide paraquat (1,1'-dimethyl-4,4'-bipyridylium dichloride). The toxicity of paraquat is due to its ability to undergo redox cycling within the cytoplasm. It is reduced to a monocation by a soluble NADPH-diaphorase and oxidized by molecular oxygen to regenerate the dication along with production of superoxide (Figure 2). Paraquat toxicity has been reported for mammals, plants, and bacteria. Within bacteria it exerts a bacteriostatic effect which has been shown to be dependent upon the presence of molecular oxygen (Kitzler and Fridovich 1987).

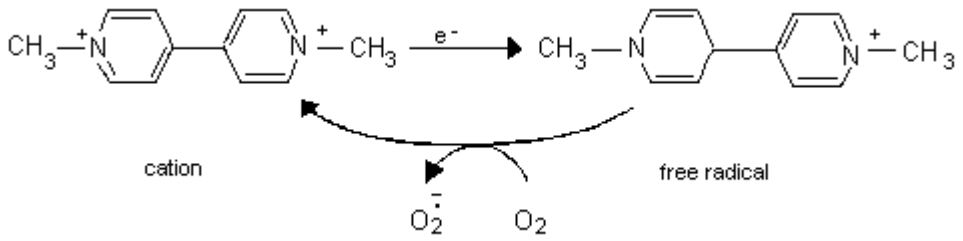

Figure 2. Paraquat redox cycling with generation of superoxide (modified from Bus and Gibson 1984).

4. SUPEROXIDE WITHIN THE PERIPLASM

A proposed source of superoxide within the periplasm of some gram-negative bacteria is the bc1 complex, a component of the respiratory chain located within the cytoplasmic membrane (Imlay 2003). Autooxidation of this complex results in reduction of molecular oxygen located within the periplasm to superoxide. Recently, superoxide production within the periplasm was detected in *E. coli* during aerobic growth (Korshunov and Imlay 2006). The bc1 complex is absent in the respiratory chain of *E. coli*; instead periplasmic superoxide production has been attributed to the autooxidation of dihydromenaquinone present within the cytoplasmic membrane.

Phagocytic cells of the innate immune system produce superoxide as part of their attack on pathogenic bacteria in a process known as the respiratory burst. Following phagocytosis of a bacterium, functional NADPH oxidases are assembled by translocation of cytosolic components of the oxidase to a membrane bound component, b cytochrome (Karlsson and Dahlgren 2002). These oxidases are formed on the plasma membrane of neutrophils as well as intracellularly on phagosomal and granule membranes. The enzyme catalyzes the oxidation of NADPH located within the cytosol and reduces molecular oxygen present in the phagosome or granule, or extracellularly in the case of

plasma membrane NADPH oxidases, to produce superoxide. Superoxide produced extracellular to a bacterium can cross the outer membrane and enter the periplasm due to the low pH of the phagolysosome. At low pH the superoxide becomes protonated, enabling diffusion (Korshunov and Imlay 2002). The respiratory burst is an essential event in phagocytic defense against invading bacteria. In individuals suffering from chronic granulomatous disease (CGD), neutrophils are unable to initiate the respiratory burst due to a defect in a subunit of NADPH oxidase, resulting in frequent bacterial and fungal infections that can be fatal (Heyworth et al. 2003).

In the lab, superoxide can be generated extracellulary with the enzyme xanthine oxidase. Xanthine oxidase is a flavoenzyme, composed of two iron-sulfur clusters, a molybdenum cofactor, and a flavin adenine dinucleotide (FAD). In humans, xanthine oxidase is involved in the catabolism of purines. It has been isolated from a wide variety of organisms, including bacteria, mice, and humans, with bovine milk being the primary commercial source since its discovery over 100 years ago (Harrison 2002). Within mammals, the enzyme can be converted to another form, called xanthine dehydrogenase, and together the two are referred to as xanthine oxidoreductase. In contrast to the dehydrogenase form, the oxidase form is only capable of reducing molecular oxygen, not NAD^+. It's most common substrates, hypoxanthine and xanthine, bind at the molybdenum site, and are oxidized to xanthine and urate respectively, with transfer of the electron to FAD resulting in reduction of molecular oxygen to form superoxide and hydrogen peroxide (Figure 3).

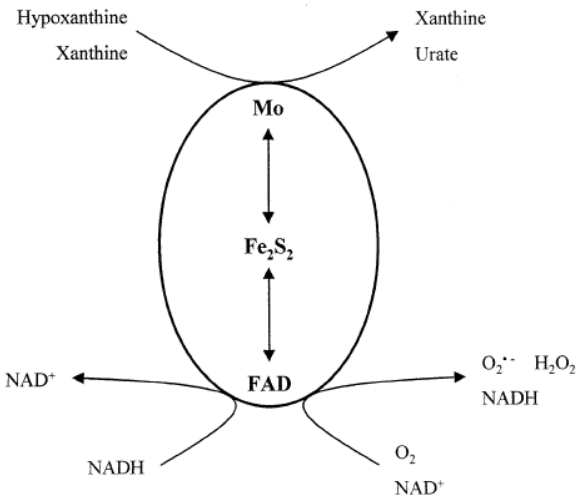

Figure 3. Production of superoxide by xanthine oxidase (Harrison 2002).

5. COMBATING SUPEROXIDE PRODUCTION: THE ROLE OF SUPEROXIDE DISMUTASE

To combat oxidative stress, aerobic organisms have enzymes that scavenge superoxide called superoxide dismutases (SODs). Isolated in 1939 from bovine erythrocytes, the enzymatic function of these proteins remained unknown until 1969 when it was discovered that they catalyzed the dismutation of superoxide to hydrogen peroxide and molecular oxygen (Equation 2).

$$O_2^- + O_2^- + 2H^+ \rightarrow H_2O_2 + O_2 \quad (2)$$

Prior to this discovery, the protein had been given different names based on the tissue from which it was isolated and the finding that it contained copper. For example, the copper-containing protein isolated from bovine erythrocytes was called erythrocuprein, from human brain tissue, cerebrocuprein, and from liver, hepatocuprein (McCord and Fridovich 1969). In 1970 and 1973 two additional forms of the enzyme were identified

in *E. coli*, with the copper-containing enzymes not identified in the species until 1994. Each form is differentiated according to the metal cofactor present at the active site: copper-zinc SOD (CuZnSOD), iron SOD (FeSOD), and manganese SOD (MnSOD).

Since their discovery, the SODs of *E. coli* have been extensively studied. The location of the three forms differs, with Fe- and MnSODs located in the cytoplasm and CuZnSODs located in the periplasm of the gram-negative bacterium. Expression of each gene is also different, with *sodB* (FeSOD) constitutively expressed, *sodA* (MnSOD) upregulated in response to oxidative stress, and *sodC* (CuZnSOD) only expressed during stationary phase (Hopkin et al. 1992). While all three are synthesized in aerobic environments, FeSODs are also synthesized in anaerobic environments where oxygen toxicity is not a threat. The synthesis of FeSODs during anaerobiosis aids facultative bacteria in transitioning from an anaerobic environment to an aerobic environment, a role evident by a two-hour growth lag observed in *E. coli sodB* mutants (Kargalioglu and Imlay 1994). The difference in the availability of iron(II) in anaerobic and aerobic environments has been suggested as an explanation as to why FeSOD rather than MnSOD is produced in an anaerobic environment and conversely why MnSOD is induced during oxidative stress in an aerobic environment and not FeSOD. Iron is more abundant in anaerobic environments than manganese and exists in its soluble +2 oxidation state. In aerobic environments it is oxidized to the insoluble ferric ion whereas manganese is soluble (Kargalioglu and Imlay 1994).

Although both Fe- and MnSODs serve to scavenge superoxide produced within the cytosol, their ability to protect different targets of superoxide from damage within *E. coli* differs. FeSODs protect superoxide-sensitive enzymes such as 6-phosphogluconate

dehydratase, while MnSODs are more efficient at protecting DNA (Hopkin et al. 1992). SODs within the cytosol reduce superoxide from the estimated production of 5 μM/s to a steady-state level of 0.1 nM (Imlay 2003). The function of periplasmic CuZnSODs has been the subject of much investigation since their discovery due to the fact that cytoplasmically generated superoxide remains in the cytosol and there are no known targets of superoxide within the periplasm. While components of the respiratory chain have been found to generate superoxide within the periplasm, the finding that *E. coli* generates periplasmic superoxide during log phase, a time during which *sodC* is not expressed, implies that CuZnSODs are not functioning to protect against damage caused by this source of superoxide (Korshunov and Imlay 2006). Given their location, it has been assumed that their primary role is scavenging superoxide generated by phagocytic immune cells, offering increased virulence to pathogenic bacteria. However, this cannot be the only role for this enzyme as CuZnSODs are produced by nonpathogenic and free living bacteria. While the concentration of CuZnSODs is much lower than Fe- and MnSODs within the cell, 0.1 nU and 12 nU respectively, it is estimated that the concentration of cytosolic SODs would have to increase by three fold to provide the same protection as CuZnSODs against superoxide entering from outside the cell (Korshunov and Imlay 2002). This implies that perhaps CuZnSODs are not protecting some unknown biomolecule within the periplasm, but are also serving to protect cytosolic targets.

6. METHODS TO ASSESS EFFECTS OF OXIDATIVE STRESS ON BACTERIA

Spectrophotometry has been the primary method employed to observe the bacteriostatic effect of superoxide generating agents such as paraquat on culture growth

rate (Kitzler and Fridovich 1986; Kitzler et al. 1990; Hassan and Fridovich 1978). With this method, absorbance readings of a liquid culture are taken at a wavelength of 600 nm at time intervals, and the absorbance reading obtained is plotted against time to construct a growth curve. This is not a true absorbance reading, as the light is not being absorbed by the bacteria, but is instead scattered; thus optical density is a more appropriate term. A drawback to this approach is that it does not differentiate between dead cells and viable cells since both are able to scatter light.

The traditional method used to assess viability of bacterial cells following treatment with a bactericidal agent is to count colony-forming units (CFUs) using the spread plate method (Hoerr et al. 2007). Typically, 100 μL of a liquid culture is spread on an agar plate and incubated at the optimum growth temperature of the bacterium to produce visible colonies evenly distributed along the surface of the agar. The range of CFUs present on a plate to achieve an accurate count is considered to be between 30 and 300. A drawback to this method is that a cell that is viable but unable to produce a colony will remain undetected. Additionally, this method is time consuming, as serial dilutions must be performed to dilute the culture and often more than one dilution must be plated to achieve the accurate range of CFUs. Furthermore, incubation time varies between species, with 24 hours to 5 days being typical (Stocks 2004).

Both viable and dead cells can be counted using a device called a hemacytometer. Although designed to count much larger blood cells, it is possible to count bacterial cells by increasing the magnification of the microscope. Larger and thicker than a standard microscope slide, a hemacytometer has two square compartments on which a grid is etched and is covered with a special coverslip to produce an area of known volume. Each

square grid is divided into 9 squares, each 1 mm^2, holding a volume of 100 nL, and is filled by capillary action. Dead cells are differentiated from live cells by using the vital stain Trypan blue, as it is unable to cross an intact membrane and therefore only stains dead cells. Cells must be diluted in phosphate buffered saline to achieve a range of 20-100 cells per square. Disadvantages of this method include difficulty in precision, as cells must be counted quickly to avoid evaporation due to heating by the light source, locating small cells, and motile cells require immobilization prior to counting. In addition, although considered a quick method, samples must often be diluted several times to achieve the optimal range of cells, with each dilution requiring a 5-15 minute incubation period with the dye to permit adequate staining. If cells are incubated with Trypan blue for too long, the dye may be taken up by viable cells.

A more rapid technique for assessing cell viability is the LIVE/DEAD BacLight Bacterial Viability Kit developed by Molecular Probes (Eugene, OR). This kit consists of two nucleic acid staining fluorescent dyes, the green fluorescent SYTO9 and the red fluorescent propidium iodide. SYTO9 is membrane permeable and can therefore stain both viable and non-viable cells, while propidium iodide is membrane-impermeable and can only stain non-viable cells. When both dyes are present in the cell, propidium iodide displaces SYTO9 due to its stronger affinity for DNA, resulting in the staining of viable cells green and non-viable cells red. Both dyes are excited by the same wavelength of light, but have different emission spectra. Only a fifteen minute incubation period is required, allowing results to be obtained quickly. Another advantage is that the kit can be adapted for use with different instrumentation, including a fluorescence microplate reader, a fluorescent microscope, a flow cytometer, or a fluorometer. In contrast to the

traditional spread-plate method, the BacLight kit allows detection of cells that are nonculturable but still viable. However, some bacterial cells, including *Bacillus clausii* and *Listeria monocytogenes*, have been reported to be stained by both dyes simultaneously, making data interpretation difficult (Stocks 2004).

SIGNIFICANCE

Since the realization just over 40 years ago that molecular oxygen can be toxic to the cell and that enzymes exist to alleviate damage caused by it, the molecular basis of oxygen toxicity and the effects it has on the cell are still not fully understood. The finding that both the innate immune system and the three major classes of bactericidal drugs rely on superoxide production as part of their attack on pathogenic bacteria highlights the need for a greater understanding of the defensive role these molecules fulfill. This understanding could lead to the development of novel therapeutic strategies to target pathogenic bacteria for which current therapies are not successful, such as the causative agent of tuberculosis, *Mycobacterium tuberculosis*. This disease remains a worldwide epidemic and is prevalent in third-world countries. Reasons include antibiotic resistance of this bacterium and its ability to detoxify reactive oxygen species released by phagocytic immune cells, an ability attributed in part to its Fe- and CuZnSODs (Ehrt and Schnappinger 2009). Given the protection provided to bacterial pathogens by superoxide dismutases, inhibition of these enzymes should make them more vulnerable to oxidative stress and increase the lethality of antibiotics and phagocytic cells. Although SOD inhibitors have been identified and utilized to understand oxygen toxicity and the role of SODs, their therapeutic application has not been explored.

SPECIFIC AIMS

The aim of this project was to explore the effects of superoxide-generating agents on growth and viability of *Escherichia coli*. The effects of endogenous and exogenous superoxide were investigated, with paraquat serving as the source of endogenous superoxide and the xanthine/xanthine oxidase (X/XO) enzyme system serving as the source of exogenous superoxide. Since previous research in the laboratory has focused on superoxide-generation using antibiotics, the bulk of the focus was given to development of the paraquat assay. Two *E. coli* strains were used in experimentation, a lab strain and a clinical isolate, to see how different strains were affected by the same conditions. For the paraquat assay, the effect of paraquat concentration, time of addition of paraquat, and culture growth medium on paraquat toxicity was explored using three different growth media: Luria-Bertani broth (LB), double strength Luria-Bertani broth (2XLB), and nutrient broth (NB). Assay development focused on conditions that resulted in a reduction of the culture growth rate by 50%. For the X/XO assay, the effect of pH on toxicity was explored using a slightly alkaline buffer (pH 7.5) and a slightly acidic buffer (pH 6.5).

During the development of oxidative stress assays, methods to assess the effect of oxidative stress on the cell were evaluated. Methods that were evaluated include: counting colony-forming units using the spread-plate method, total cell counts with a hemacytometer, cell density measurements taken with a spectrophotometer, and fluorescence measurements taken with a fluorescence microplate reader using the LIVE/DEAD BacLight Bacterial Viability Kit manufactured by Molecular Probes. Each

method was evaluated by comparison of the treated culture with an untreated culture grown in parallel. Optimization of the BacLight kit for each *E. coli* strain is an important objective, as the kit will be essential for future high-throughput screening of potential SOD inhibitors.

Following development of the paraquat assay, the CuZnSOD inhibitor diethyldithiocarbamate (DDC) was used to investigate the effects of SOD inhibition on culture growth. The primary focus was to identify a concentration of DDC that reduces culture growth rate in the optimum conditions identified for the paraquat assay. Although paraquat generates superoxide in the cytosol and DDC inhibits periplasmic SODs, this assay was important in assessing the effects of simultaneously subjecting the cell to both periplasmic superoxide generated by autooxidation of electron carriers within the respiratory chain and cytoplasmic superoxide. Once reduction in culture growth rate was achieved by DDC alone, cells were treated with both DDC and paraquat simultaneously and the effect on growth rate evaluated.

MATERIALS AND METHODS

1. MAINTENANCE OF *E. COLI* STRAINS

Prior to this project, the *E. coli* strain ER2566 (IMPACT kit, New England BioLabs Inc., Ipswhich, MA) was stored as a stab culture at 4^{o}C. The clinical isolate, ATCC 4157 (MicroBioLogics, Saint Cloud, MN) was rehydrated from a freeze-dried culture according to the manufacturer's protocol. Once rehydrated, a serial dilution was performed and isolated colonies obtained using the spread-plate method (Figure 4). A stab culture was prepared from an isolated colony and stored at 4^{o}C protected from light. Isolated colonies were maintained on Luria-Bertani agar plates (100 x 15 mm) using the streak-plate technique followed by inversion of plates and incubation at 37^{o}C overnight in a Lab-Line L-C Incubator (Melrose Park, IL). Liquid cultures were grown from isolated colonies in a Series 25 Incubator Shaker (New Brunswick Scientific Co, Edison, NJ) at 37^{o}C and a shake speed of 200 rpm. Media recipes for Luria-Bertani broth, double strength Luria-Bertani broth, and nutrient broth are located in the appendix.

2. GROWTH CURVES

Overnight cultures were diluted 1:200 in pre-warmed growth medium in 13 x 100 mm borosilicate glass disposable culture tubes to a total volume of 4 mL. Tubes were covered with parafilm and placed in the Series 25 Incubator Shaker at 37^{o}C and 200 rpm. Optical density (OD) measurements were taken at a wavelength of 600 nm with a Spectronic 20+ spectrophotometer (Thermo Electron Corporation). Readings were taken at 30 minute intervals, and the tube vortexed briefly prior to placement into the sample

compartment. Due to the ability of *E. coli* cells to form chains and clump, a 45 second delay between placement of the tube in the sample compartment and recording of the OD reading was necessary to allow the needle to steady.

3. PARAQUAT ASSAY

Overnight cultures were diluted 1:200 in pre-warmed growth medium in 13 x 100 mm borosilicate glass disposable culture tubes. Paraquat solutions 100X the final desired concentration were prepared by dissolving the solid in sterile water. Each tube contained 3,940 μL of fresh growth medium and 20 μL of overnight culture. The final volume of each tube was 4 mL, with treated cultures receiving 40 μL of the paraquat solution (1:100) and untreated cultures receiving 40 μL of sterile water. Optical density measurements (600 nm) were taken every 30 minutes as described in section 2.

4. SPREAD-PLATE METHOD

A 10 μL aliquot was removed from the culture tube and serially diluted in 2 mL microcentrifuge tubes containing 0.85% NaCl solution as outlined in Figure 4. The samples were plated onto LB agar plates by pipetting 100 μL of the sample onto the center of the plate. The solution was spread evenly on the surface of the agar using sterile EZ-Spread Plating Beads (Genlantis, San Diego, CA). The plates were set aside for a few minutes to allow the solution to soak into the agar, followed by wrapping parafilm around the outside edge of the plates, inversion of the plates, and placement of plates into the incubator at 37^{o}C.

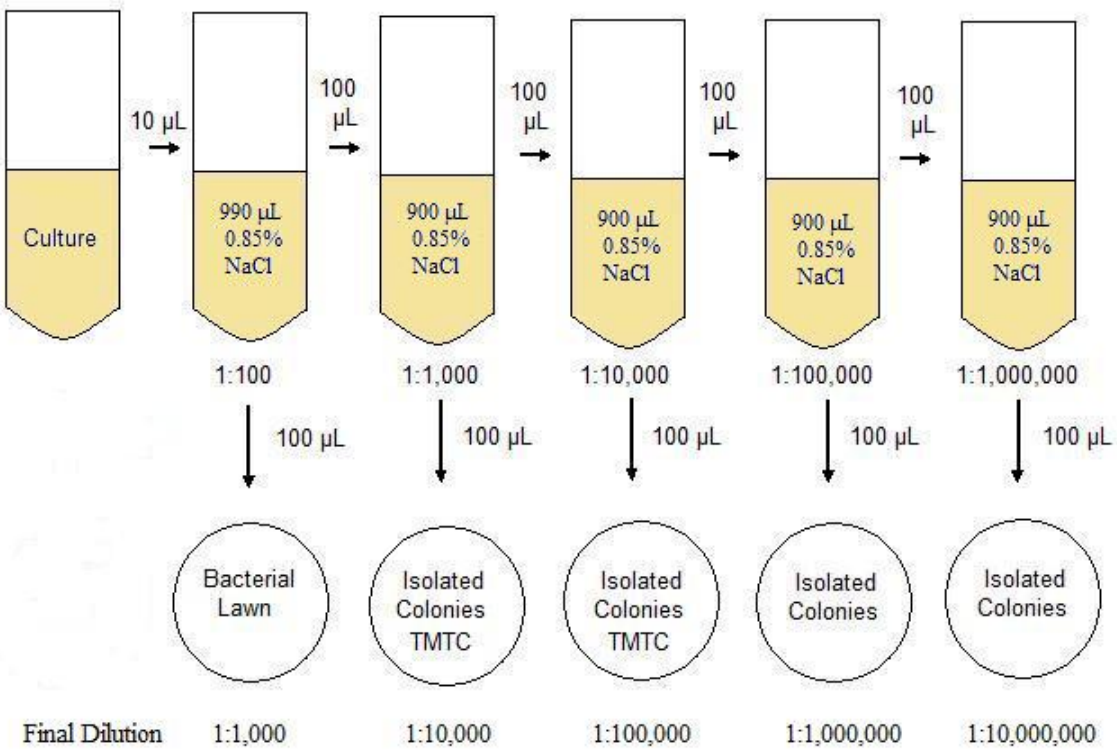

Figure 4. Outline of spread-plate method. Plates having over 300 colonies were recorded as too many to count (TMTC).

5. HEMACYTOMETER COUNTS

A 200 µL aliquot of the cell culture was diluted 1:5 with 500 µL of Trypan blue stain and 300 µL of phosphate buffered saline (PBS) in a 2 mL microcentrifuge tube. Tubes were vortexed and incubated at room temperature for 5-15 minutes. Prior to use, the hemacytometer and coverslip were cleaned with 70% isopropanol. Chambers were filled by capillary action by placing the solution filled pipette tip at the loading groove at the edge of the coverslip, with each chamber holding approximately 20 µL of cell suspension. The slide was placed on the microscope stage and the grid focused at 100X magnification, allowing observation of one grid at a time. Once focused, magnification

was increased to 400X allowing viewing of 1 square at a time to enable counting. Five of the nine squares were counted, the 4 corner squares and the center square (Figure 5). If fewer than 20 or more than 100 cells were present per square, the dilution factor was adjusted. Both grids were counted, and the average number of cells per square calculated by dividing the sum of the number of cells by 10. The number of cells per mL was calculated according to Equation 3.

average cell count per square x dilution factor x 10^4 = bacterial cells/mL (3)

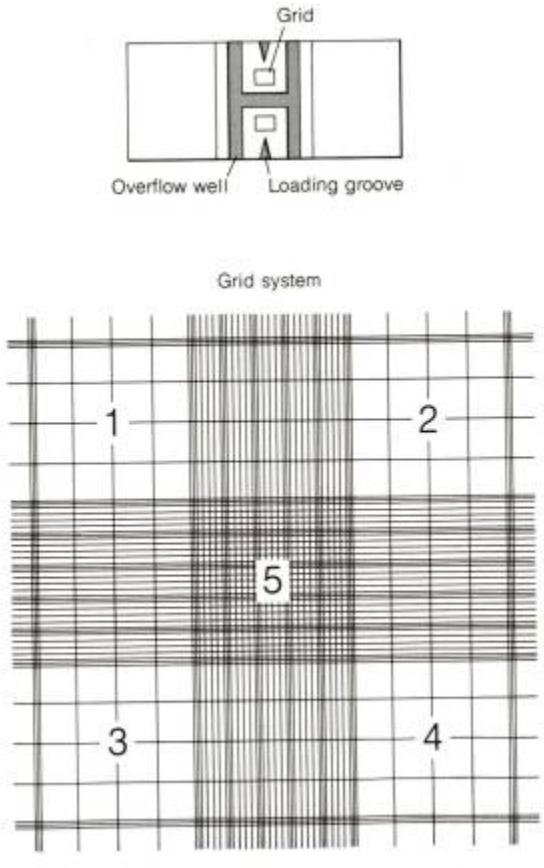

Figure 5. Sections of a hemacytometer (above) and grid system (below) for cell counting, with squares counted numbered 1-5 (Mishell and Shiigi 1980).

6. LIVE/DEAD BACLIGHT BACTERIAL VIABILITY KIT

Optimization of SYTO9

To optimize staining, SYTO9 was first calibrated for each strain by testing a range of concentrations. Cells were harvested in late log phase, a point at which they can be assumed to be 100% live, by centrifugation at 4300 rpm at 4^{o}C using a Sorvall RC 5C Plus centrifuge with rotor SH-3000 (Dupont). Following centrifugation, cells were washed in 0.85% NaCl solution to remove growth medium. Cells were resuspended in the salt solution and the optical density adjusted to the appropriate reading for the strain to be stained by adding more 0.85% NaCl as necessary. To prepare a range of SYTO9 concentrations for testing, a concentrated solution was prepared by dilution of the 3.34 mM stock solution supplied in the kit in sterile water. From this concentrated solution, a serial dilution was performed to achieve a concentration range 2X that of the desired final concentration. Each dye concentration was diluted 1:1 with cells in separate wells of a black flat-bottom 96-well microplate (Costar 3915) for a total volume of 200 μL per well (100 μL cells + 100 μL dye solution). Following incubation of the plate at room temperature in the dark for 15 minutes, fluorescence measurements were taken using a fluorescence microplate reader (POLARstar OPTIMA, BMG Labtech) with the excitation wavelength set to 485 nm and the emission wavelength set to 520 nm. A plot of green fluorescent intensity versus dye concentration was used to determine the optimum dye concentration.

Optimization of Propidium Iodide

Following optimization of the SYTO9 concentration, propidium iodide was calibrated by testing a range of dye concentrations while keeping the concentration of SYTO9 constant. Cells were prepared for staining according to the manufacturer's protocol (Molecular Probes) outlined in Figure 6. Cells were harvested using a Sorvall RC 5C Plus centrifuge (Dupont).

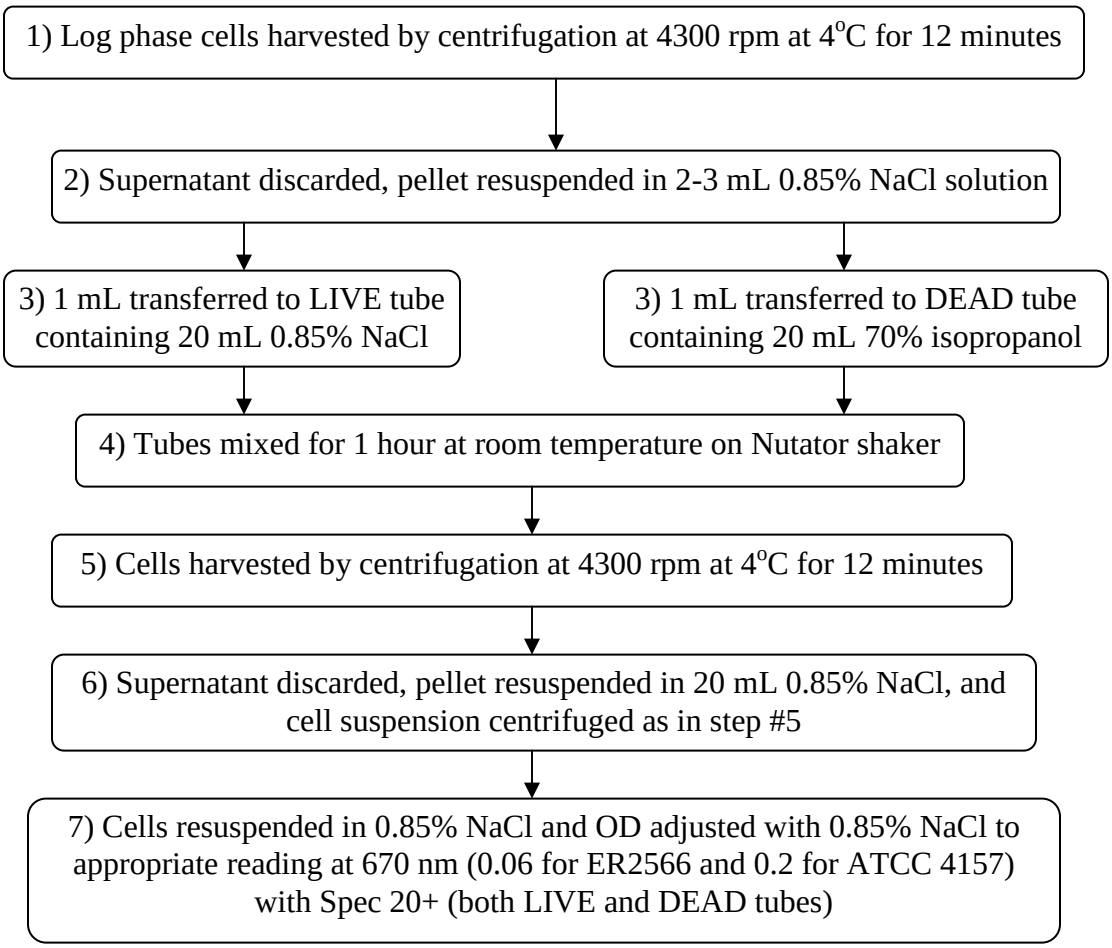

Figure 6. Protocol for preparation of cells for staining with BacLight kit.

Once both 100% live and 100% dead cultures were adjusted to the appropriate optical density, 5 different ratios of live to dead cells were prepared by mixing different proportions of live and dead cell suspensions to a total volume of 2 mL. The 5 different ratios of live to dead cells prepared were as follows: 0:100 (0% live), 10:90 (10% live), 50:50 (50% live), 90:10 (90% live), and 100:0 (100% live). A concentrated solution of propidium iodide was prepared from the 20 mM stock supplied in the kit by dilution in water. From this concentrated solution, a serial dilution was performed to achieve a concentration range 4X that of the desired final concentration. Each dye concentration was diluted 1:1 with a solution of SYTO9 4X its determined optimal concentration. Each dye mixture was diluted 1:1 with cells in separate wells of a black flat-bottom 96-well microplate (Costar 3915) for a total volume of 200 μL per well (100 μL cells + 100 μL dye mixture). Following incubation of the plate at room temperature in the dark for 15 minutes, fluorescence measurements were taken using a fluorescence microplate reader (POLARstar OPTIMA, BMG Labtech) with the excitation wavelength set to 485 nm and dual emission at 520 nm and 612 nm.

Fluorescence Measurements with DAPI nucleic acid stain

ER2566 cells in late log phase were harvested by centrifugation at 4300 rpm at 4^{o}C for 12 minutes using a Sorvall RC 5C Plus centrifuge, followed by a wash step in 0.85% NaCl solution. The pellet was resuspended in 0.85% NaCl solution and the optical density adjusted to 0.06 at 670 nm using a Spec 20+ spectrophotometer. A 2 mL working solution (10 μg/mL) of DAPI (4',6-diamidino-2-phenyl-indole) was prepared by diluting 4 μL of the stock solution 1:500 in phosphate buffered saline (PBS). Using an

Impact^2 electronic pipette (Matrix, Hudson, NH), 1 mL of cell suspension was drawn into the pipette tip, and 200 μL dispensed into 5 consecutive wells within a row of a black flat-bottom 96-well microplate (Costar 3915). This step was repeated to fill the next 5 consecutive wells. In the next row, 200 μL of cell suspension was transferred into 10 consecutive wells with a manual pipetter. Each well then received 50 μL of DAPI working solution for a final dye concentration of 2 μg/mL per well. The plate was covered and incubated at room temperature overnight. Fluorescent intensity was measured with a fluorescence microplate reader (POLARstar OPTIMA, BMG Labtech), with the excitation wavelength set at 360 nm and emission wavelength at 460 nm.

Absorbance Test for Inner Filter Effects

Cells were prepared as described above for staining with both SYTO9 and propidium iodide, with 3 different ratios of live to dead cells prepared: 100% live, 50% live, and 0% live. From the stock solutions provided in the LIVE/DEAD BacLight Bacterial Viability Kit, 450 μL of each dye and 450 μL of dye mixture (SYTO9 + PI) was prepared each having a dye concentration 2X the final desired concentration by dilution of the stocks in sterile water. One hundred μL of each live to dead ratio was plated in triplicate within the same row in a clear flat bottom 96-well plate (Nunc F, Nalge Nunc International, Rochester, NY), resulting in 3 columns each containing one of each live:dead cell suspension. One column received 100 μL of SYTO9, one column 100 μL of PI, and one column 100 μL dye mixture. In a fourth column, 100 μL of each dye and dye mixture was plated without cells in 100 μL of 0.85% NaCl solution. Absorbance measurements were taken at a wavelength of 485 nm, 520 nm, and 612 nm using a

microplate reader spectrophotometer (SpectraMax 190, Molecular Devices, Sunnyvale, CA).

7. XANTHINE/XANTHINE OXIDASE ASSAY

Cells were grown until stationary phase and harvested by centrifugation at 4300 rpm at 4^{o}C for 12 minutes in a Sorvall RC 5C Plus centrifuge. Cells were resuspended in 50 mM potassium phosphate buffer (PPB) and the optical density was adjusted to 0.3 at 670 nm with a Spec 20+ (Thermo Electron Corporation, Waltham, MA). The pH of PPB was adjusted to 6.5 with 1 N HCl or 7.5 with 1 N KOH. A 0.15 mM xanthine solution was prepared by dissolving the solid in 1 mL 1 N NaOH followed by addition of sterile water and adjustment to the desired pH with 1 N HCl for a final volume of 100 mL. One hundred μL of xanthine oxidase enzyme solution (XO) containing 0.2 units/mL was prepared by dilution of the stock (0.2 units/mg protein, 51 mg protein/mL) xanthine oxidase suspension (Sigma, St. Louis, MO) in cold PPB. A 3 mL reaction mix was prepared for both treated and untreated cultures by adding 1.9 mL of the cell suspension and 1 mL of xanthine solution to a culture tube. Treated cultures received 100 μL of XO while untreated tubes received 100 μL of sterile water. Tubes were vortexed and placed on the Nutrator mixer. For the LIVE/DEAD assay, 100 μL aliquots were removed at 0, 30, 60, 90, and 120 minute time intervals and cells harvested by centrifugation in a microcentrifuge for 5 minutes at 14,000 rpm. The pellets were resuspended in 0.85% NaCl solution and the optical density adjusted to 0.06 at 670 nm. For the spread-plate method, 10 μL aliquots were removed at each time point.

8. SOD INHIBITION WITH DIETHYLDITHIOCARBAMATE (DDC)

DDC Concentration Determination

Overnight cultures were diluted 1:200 in pre-warmed nutrient broth in 13 x 100 mm borosilicate glass disposable culture tubes. A DDC solution 100X the desired final concentration (2 mM) was prepared by dissolving the solid in sterile water. Each tube contained 3,940 μL of fresh growth medium and 20 μL of overnight culture. The final volume of each tube was 4 mL, with treated cultures receiving 40 μL of the DDC solution (1:100) and untreated cultures receiving 40 μL of sterile H_2O. Optical density measurements (600 nm) were taken every 30 minutes as described in section 2.

DDC and Paraquat Combination Treatment

Overnight cultures were diluted 1:200 in pre-warmed nutrient broth in 13 x 100 mm borosilicate glass disposable culture tubes. Four cultures were grown in parallel in a Series 25 Incubator Shaker set at a temperature of 37^{o}C and shaking at 200 rpm. These included: untreated culture, paraquat only treated culture, DDC only treated culture, and paraquat + DDC treated culture. Paraquat and DDC solutions were prepared as described above, with both 100X and 200X solutions prepared for final concentrations of 1 mM for paraquat and 20 μM for DDC. Each tube contained a total volume of 4 mL, with tubes prepared according to Table 1. Tubes were removed from the incubator shaker at 30 minute time intervals and optical density readings taken at 600 nm with a Spec 20+ spectrophotometer.

Table 1. Preparation of tubes for SOD inhibition assay.

Tube	**Contents**
Untreated	3,940 μL NB 20 μL overnight culture 40 μL water
DDC Treatment	3,940 μL NB 20 μL overnight culture 40 μL 100X DDC solution
Paraquat Treatment	3,940 μL NB 20 μL overnight culture 40 μL 100X PQ^{2+} solution
Paraquat/DDC Treatment	3,940 μL NB 20 μL overnight culture 20 μL 200X DDC solution 20 μL 200X PQ^{2+} solution

RESULTS

1. CELL DENSITY MEASUREMENTS WITH A SPECTROPHOTOMETER

Cell Density as a Measurement of Growth: Construction of Growth Curves

Both *E. coli* strains exhibited similar growth patterns, entering stationary phase at around 5 hours of growth (Figures 7 & 8). By switching from inoculation with an isolated colony to inoculation with an overnight culture, the lag phase for ER2566 was shortened from 2 hours to 30 minutes (data not shown).

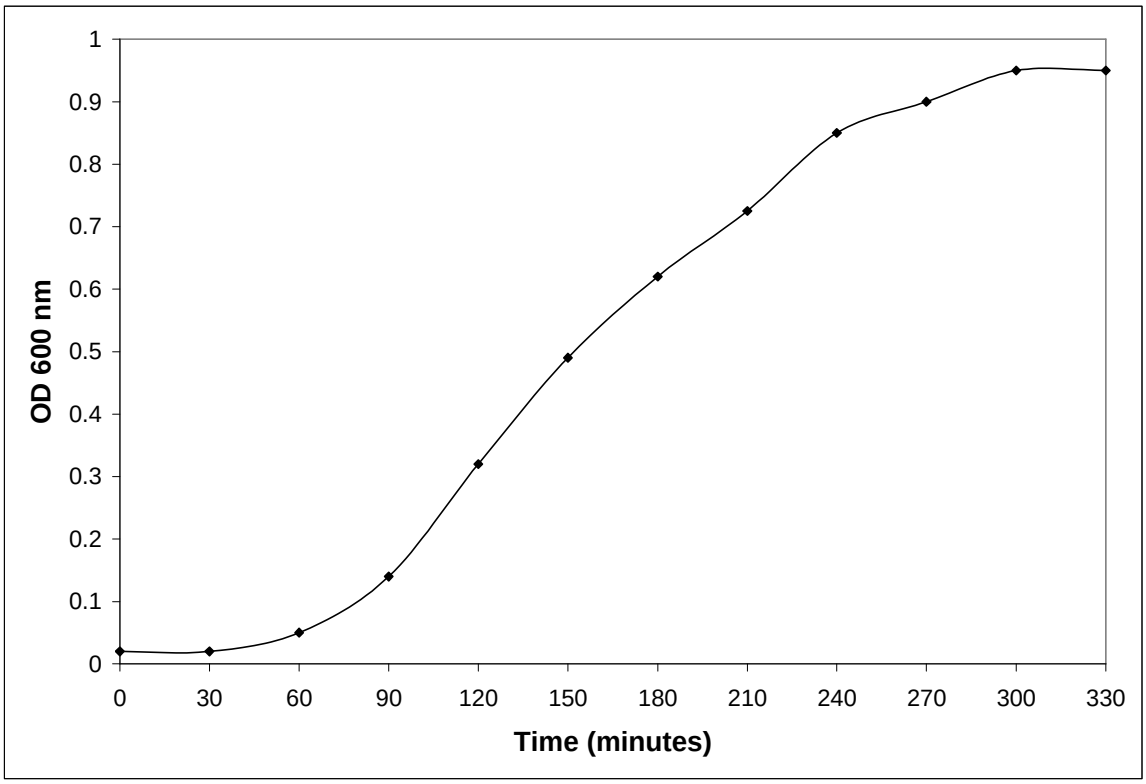

Figure 7. ER2566 Growth Curve. Overnight cultures were diluted 1:200 in 4 mL fresh Luria-Bertani broth. Optical density measurements were taken at 30 minute intervals with a Spec 20+ spectrophotometer.

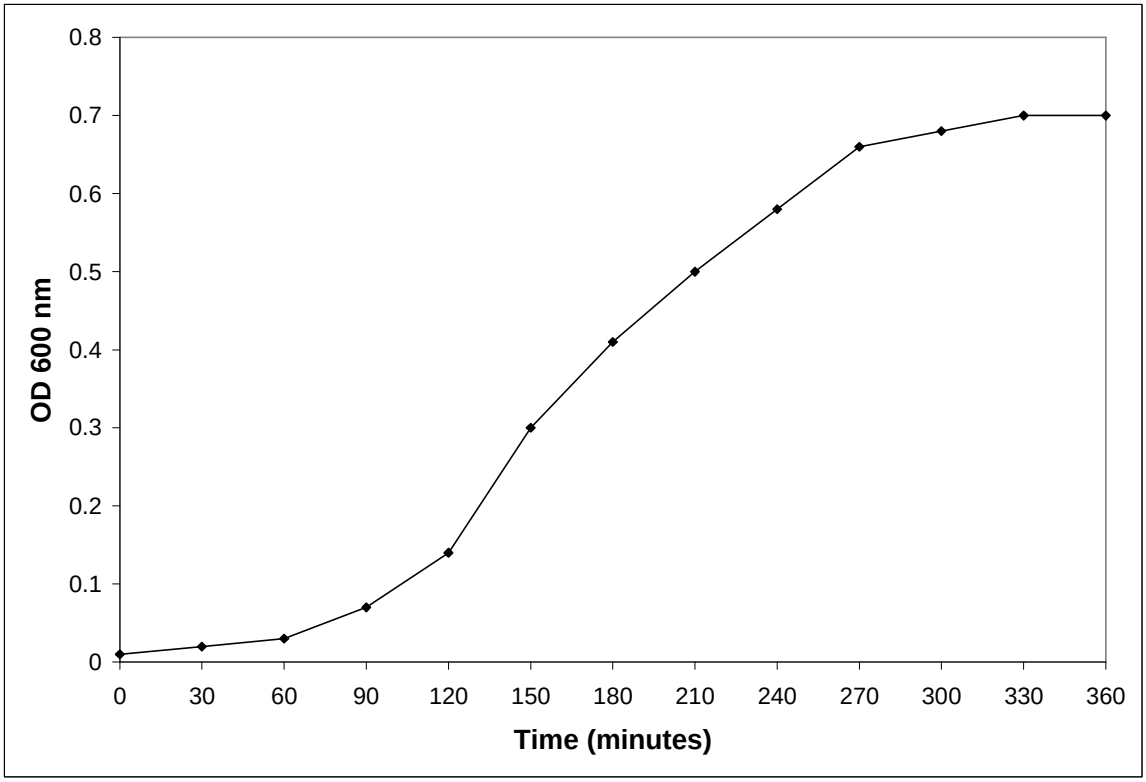

Figure 8. ATCC 4157 Growth Curve. Overnight cultures were diluted 1:200 in 4 mL fresh Luria-Bertani broth. Optical density measurements were taken at 30 minute intervals with a Spec 20+ spectrophotometer.

Relationship Between Optical Density and CFUs

The accepted standard conversion factor for relating optical density measurements to cell number for *E. coli* is OD_{600} 0.1= 10^8 cells/mL. However, this conversion can differ between strains due to differences between lipopolysaccharides attached to the outer membrane. In addition, the composition of lipopolysaccharides may change due to changes in growth conditions; therefore, it was necessary to calibrate the optical density measurements for each strain for both log and stationary phases (Raetz and Whitfield 2002). Linear regression was performed on plots of CFUs/mL vs. OD_{670} to determine the relationship between colony-forming units and optical density at 670 nm. The number of colony-forming units per mL was determined using the spread-plate method. As shown

in Figures 9-12, different relationships were found for each strain, as well as for different growth stages for the same strain. The conversion factors from OD_{670} to CFUs/mL determined for each strain and for both growth stages are shown in Table 2. Only log phase ATCC 4157 cells were found to have a conversion factor equal to the standard conversion factor found in the literature for *E. coli*.

Table 2. List of OD_{670} to CFUs/mL conversion factors for ER2566 and ATCC 4157

Strain	**Growth Phase**	**Conversion Factor Between OD_{670} and CFUs/mL**
ER2566	Log Phase	OD_{670} 0.1 = 10^7 CFUs/mL
	Stationary Phase	OD_{670} 0.1 = 9 x 10^6 CFUs/mL
ATCC 4157	Log Phase	OD_{670} 0.1 = 10^8 CFUs/mL
	Stationary Phase	OD_{670} 0.1 = 3 x 10^7 CFUs/mL

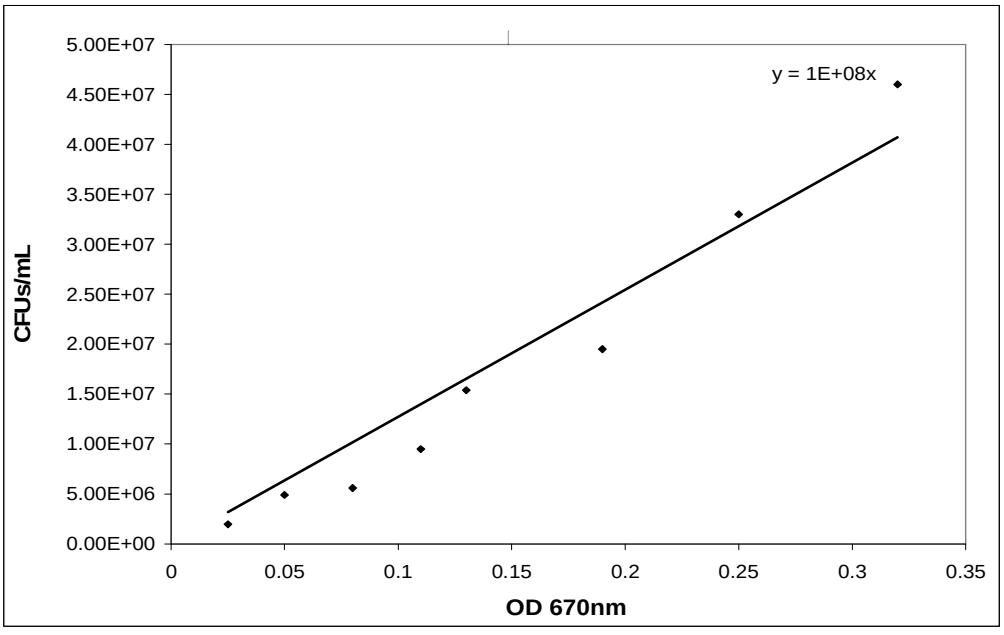

Figure 9. Relationship between optical density measurements at 670 nm and colony-forming units for log phase ER2566.

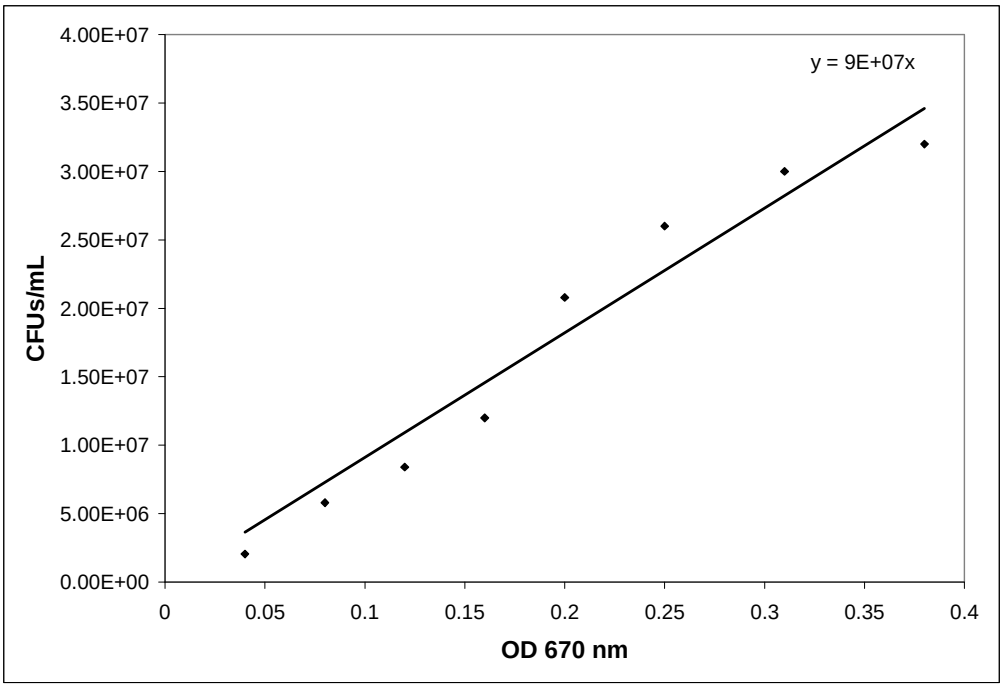

Figure 10. Relationship between optical density measurements at 670 nm and CFUs/mL for stationary phase ER2566.

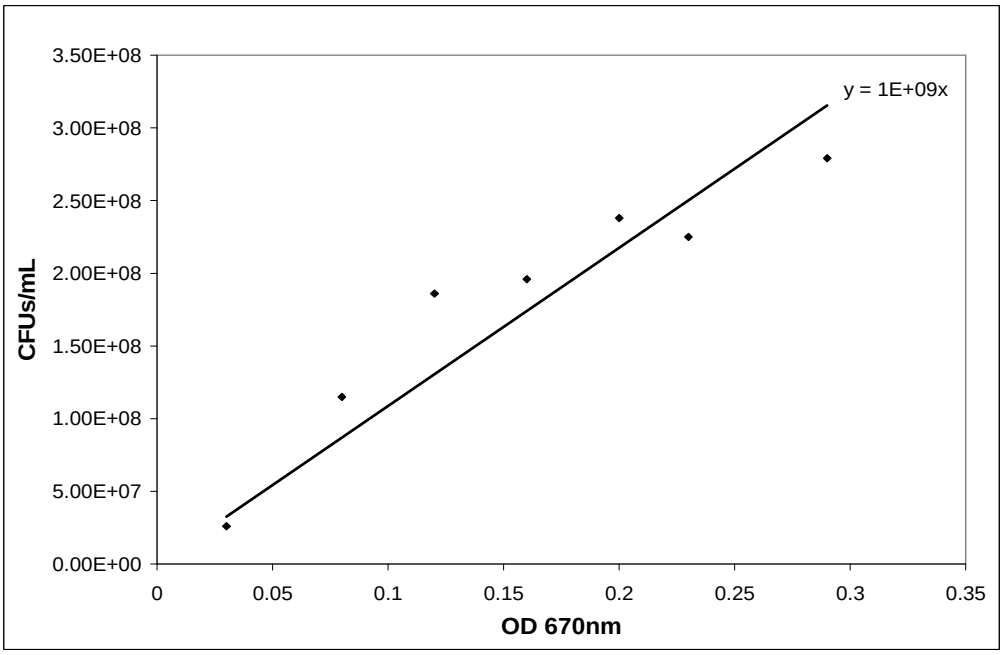

Figure 11. Relationship between optical density measurements at 670 nm and CFUs/mL for log phase ATCC 4157.

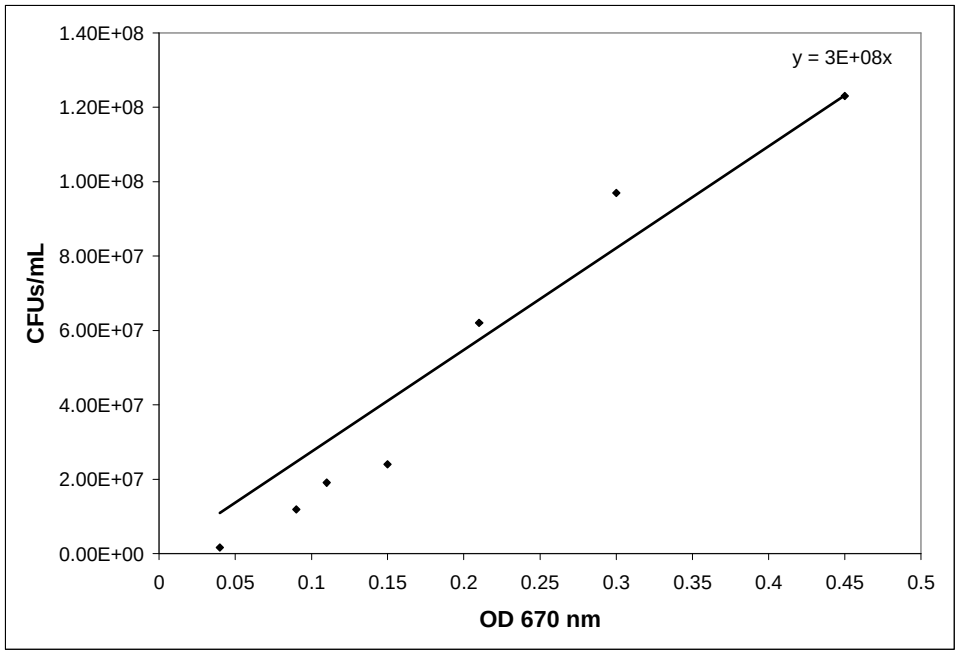

Figure 12. Relationship between optical density measurements at 670 nm and CFUs/mL for stationary phase ATCC 4157.

Relationship Between Optical Density Measurements and Total Cell Count

To take into account both dead cells and nonculturable viable cells when determining the number of cells from optical density measurements, total cell counts were made using a hemacytometer for a range of optical density measurements at 670 nm. This was done for both *E. coli* strains as well as log and stationary phases for each strain. As Figures 13-16 show, a different relationship between optical density measurements and total cell count was obtained for each strain and each growth phase. The relationships were also different from those obtained using colony-forming unit counts. For both ER2566 and ATCC 4157, less than 5% of log phase cells were found to be dead for each optical density measurement and were omitted from the graphs for clarity. For stationary phase cells, the number of dead cells increased with increased cell density, but remained less than 20% of the total cell count. The conversion factors from

OD_{670} to total cell counts are shown in Table 3. As with CFU/mL, a linear relationship was only obtained for optical density measurements below 0.45.

Table 3. List of OD_{670} to cells/mL conversion factors for ER2566 and ATCC 4157

Strain	**Growth Phase**	**Conversion Factors between OD_{670} and Cells/mL**
ER2566	Log Phase	OD_{670} 0.1 = 4 x 10^6 Cells/mL
	Stationary Phase	OD_{670} 0.1 = 5 x 10^6 Cells/mL
ATCC 4157	Log Phase	OD_{670} 0.1 = 3 x 10^6 Cells/mL
	Stationary Phase	OD_{670} 0.1= 2 x 10^7 Cells/mL

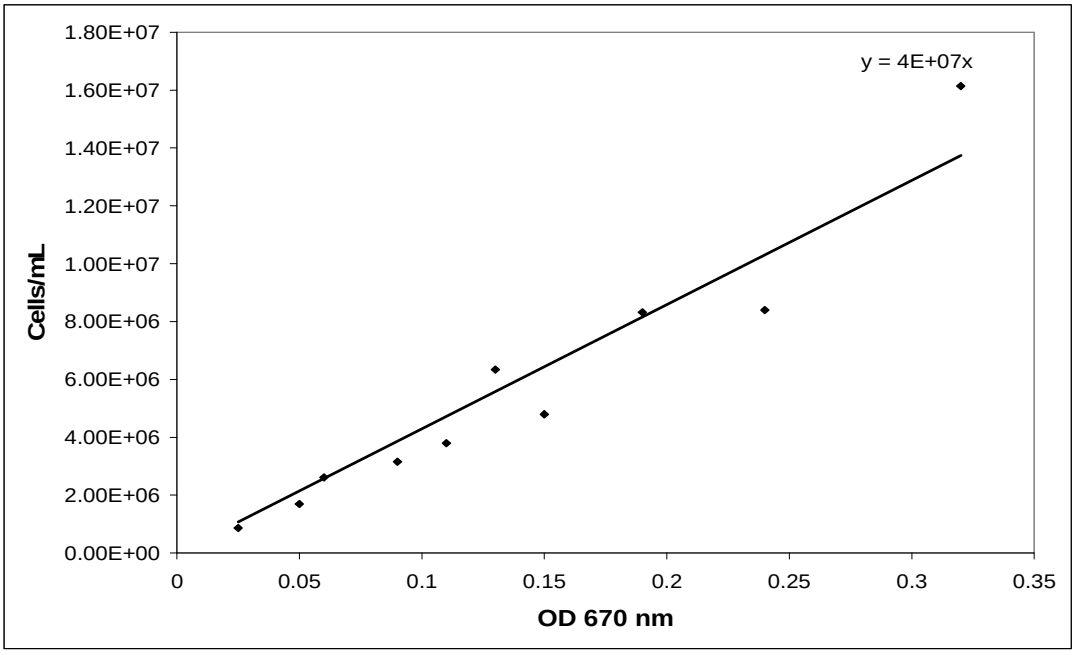

Figure 13. Relationship between total cell count and optical density measurements at 670 nm for log phase ER2566.

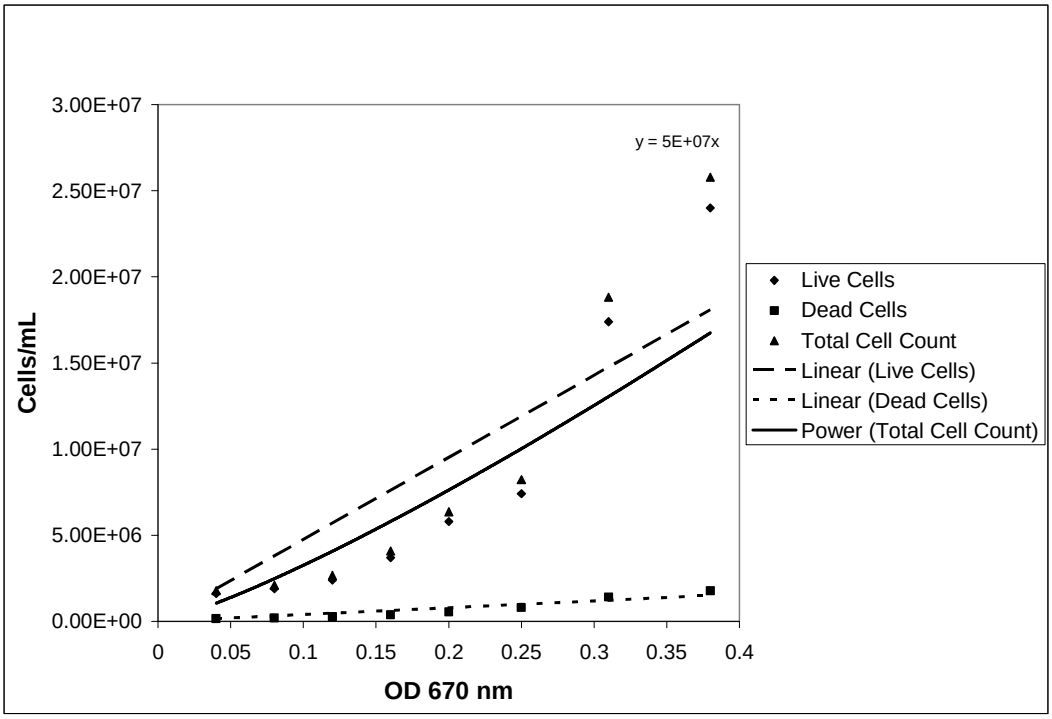

Figure 14. Relationship between total cell count and optical density measurements at 670 nm for stationary phase ER2566.

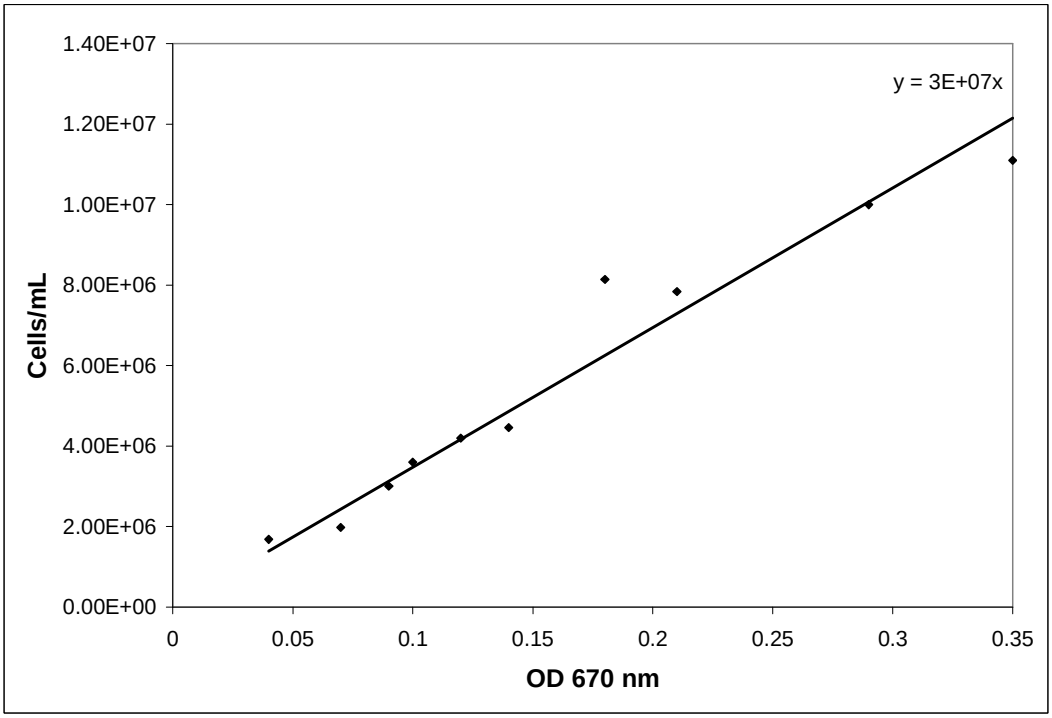

Figure 15. Relationship between total cell count and optical density measurements at 670 nm for log phase ATCC 4157.

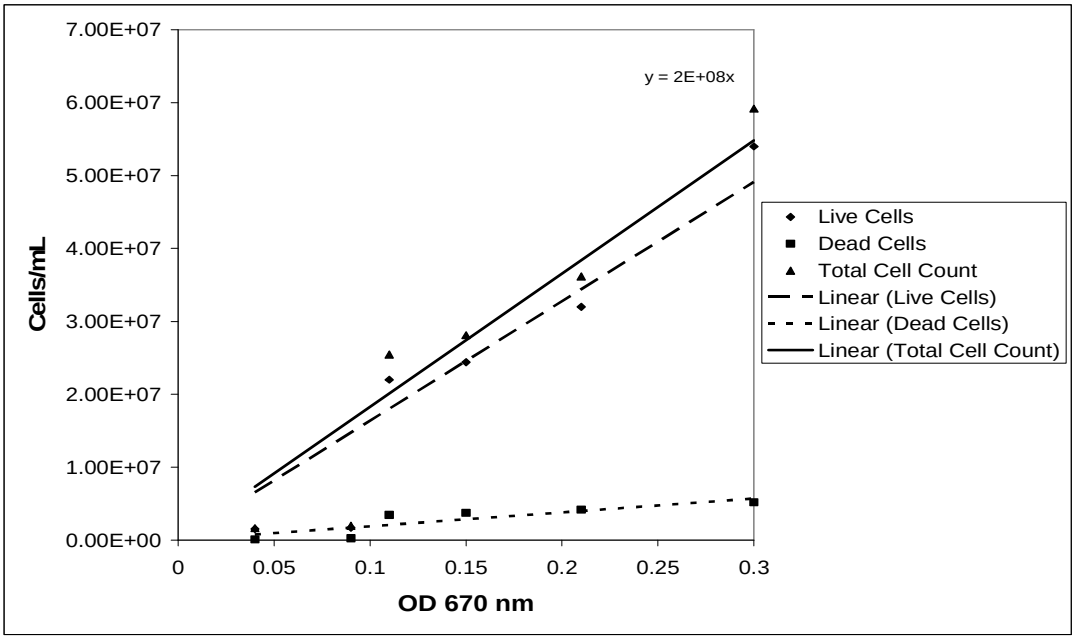

Figure 16. Relationship between total cell count and optical density measurements at 670 nm for stationary phase ATCC 4157.

2. DEVELOPMENT OF THE PARAQUAT ASSAY

Effect of Paraquat on Growth Rate of ER2566

After performing a literature search of concentrations of paraquat previously used to induce oxidative stress in *E. coli*, paraquat concentrations ranging between 1 μM and 1 mM were tested to assess the effect each had on the growth rate of ER2566 (data not shown) (Hassan and Fridovich 1978; Carr et al. 1986; Kitzler et al. 1990). Based on these experimental results, a narrower range was chosen for further investigation. Luria-Bertani broth was chosen as the growth medium since it has been considered to be the standard medium for *E. coli* cultivation since its formulation in 1951. As shown in Figure 17, all three paraquat concentrations tested reduced culture growth rate. For cultures treated with 0.5 mM and 0.75 mM paraquat, a decrease in optical density measurements occurred 90 minutes after treatment with paraquat. This decrease occurred

for a longer period and was more pronounced for the 0.75 mM paraquat treated culture (Figure 17). From this data, a paraquat concentration of 0.5 mM was chosen for ER2566 cultured in LB due to the reduction in culture growth rate greater than 50%.

To assess the effects of time of addition of paraquat on its toxicity, 0.5 mM paraquat was added to ER2566 growing in LB 60, 90, and 120 minutes following inoculation with overnight culture. As shown in Figure 18, no effect on culture growth rate was observed when paraquat was added at 90 and 120 minutes. When added at 60 minutes, a time at which the culture was still in lag phase, 0.5 mM paraquat treatment reduced culture growth rate by more than 50% as previously observed. This indicated that paraquat must be added to the culture before it enters log phase in order to exert a bacteriostatic effect. Treating log phase cells with 4 mM and 8 mM paraquat confirmed this, as no effect on culture growth rate was observed (Figure 19).

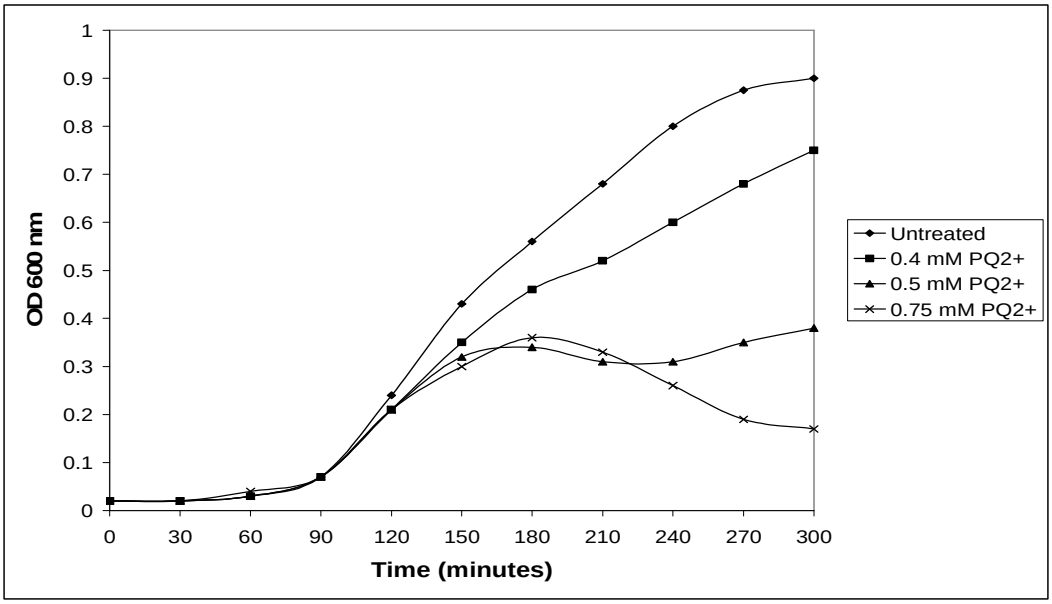

Figure 17. Effect of paraquat on growth rate of ER2566. Untreated and treated cultures were grown in parallel in 4 mL LB. Separate treated cultures received 40 μL of 0.4, 0.5, and 0.75 mM paraquat 60 minutes following inoculation and untreated culture received 40 μL of sterile H_2O. Optical density measurements were taken at 30 minute intervals at a wavelength of 600 nm with a Spec 20+.

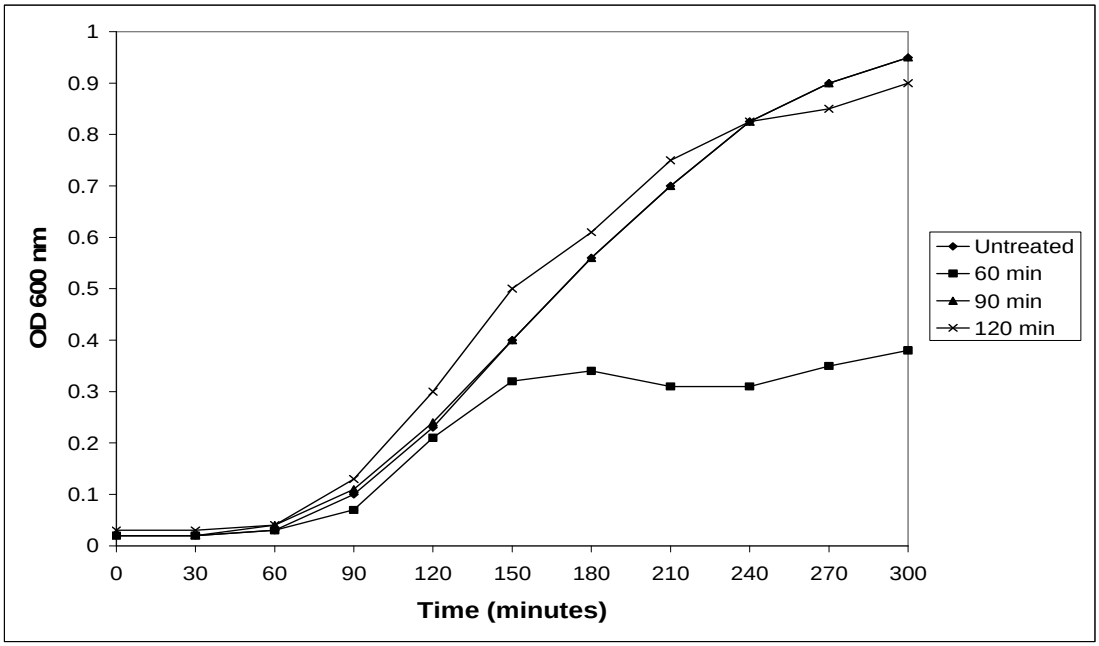

Figure 18. Effect of 0.5 mM paraquat on growth rate of ER2566 cultured in LB. Untreated and treated cultures were grown in parallel in 4 mL LB. Separate treated cultures received 40 µL of 0.5 mM paraquat 60, 90, 120 minutes following inoculation and untreated culture received 40 µL of sterile H_2O. Optical density measurements were taken at 30 minute intervals at a wavelength of 600 nm with a Spec 20+.

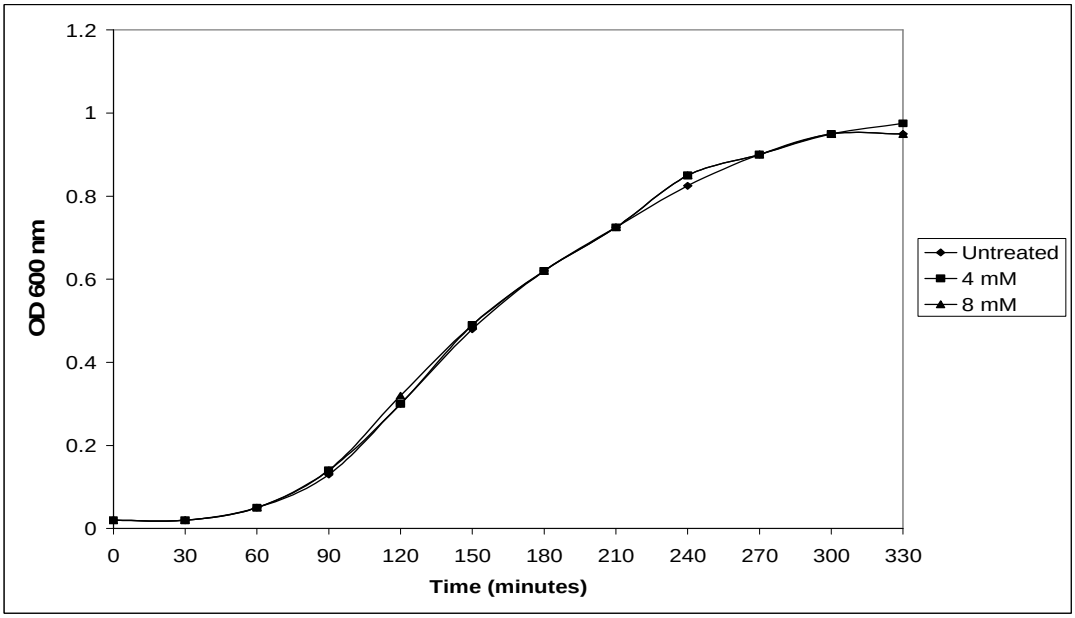

Figure 19. Effect of high paraquat concentrations on growth rate of ER2566. Untreated and treated cultures were grown in parallel in 4 mL LB. Separate treated cultures received 40 µL of 4 mM and 8 mM paraquat 120 minutes following inoculation and untreated culture received 40 µL of sterile H_2O. Optical density measurements were taken at 30 minute intervals at a wavelength of 600 nm with a Spec 20+.

To examine the effects of growth medium on paraquat toxicity, cells cultured in double strength Luria-Bertani broth (2XLB) and nutrient broth (NB) were subjected to treatment with 1 mM paraquat. As shown in Figure 20, 1 mM paraquat had no effect on culture growth rate when ER2566 cells were cultured in 2XLB even when added to the culture as early as 30 minutes following inoculation when the culture was still in lag phase. In contrast, when cultured in NB, 1 mM paraquat reduced culture growth rate at all three times tested, with a 50% reduction occurring when added at 120 minutes following inoculation when cells were in log phase (Figure 21). A reduction greater than 50% occurred when paraquat was added 60 and 90 minutes following inoculation. These results indicate that growth medium can alter the bacteriostatic effect of paraquat.

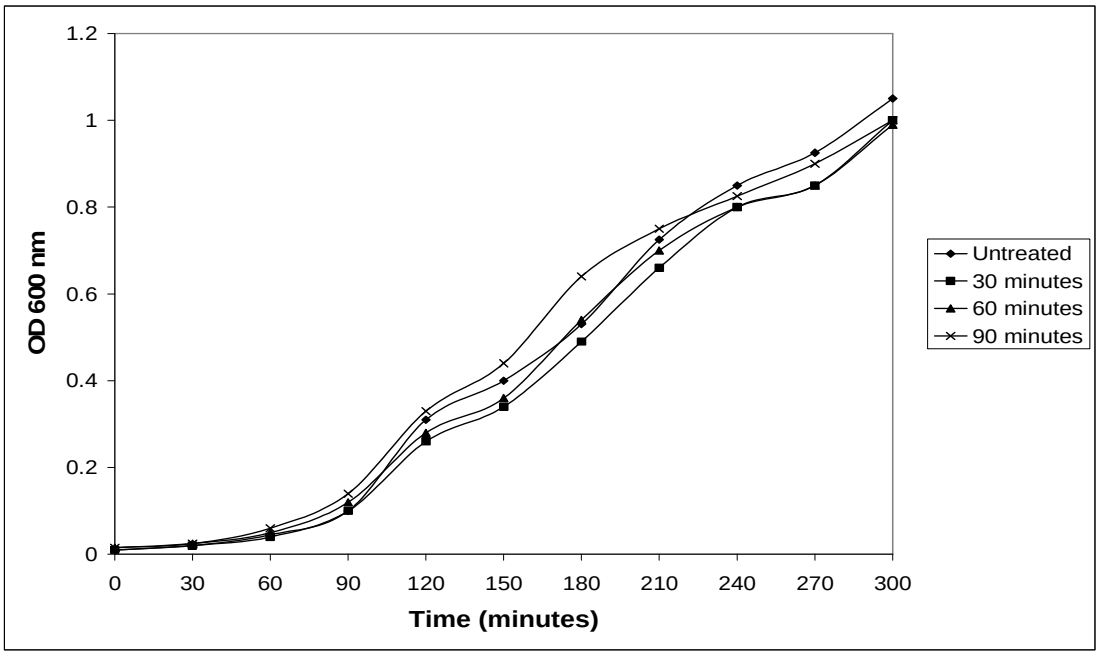

Figure 20. Effect of 1 mM paraquat on growth rate of ER2566 cultured in 2XLB. Untreated and treated cultures were grown in parallel in 4 mL 2XLB. Separate treated cultures received 40 μL of 1 mM paraquat 30, 60, and 90 minutes following inoculation and untreated culture received 40 μL of sterile H_2O. Optical density measurements were taken at 30 minute intervals at a wavelength of 600 nm with a Spec 20+.

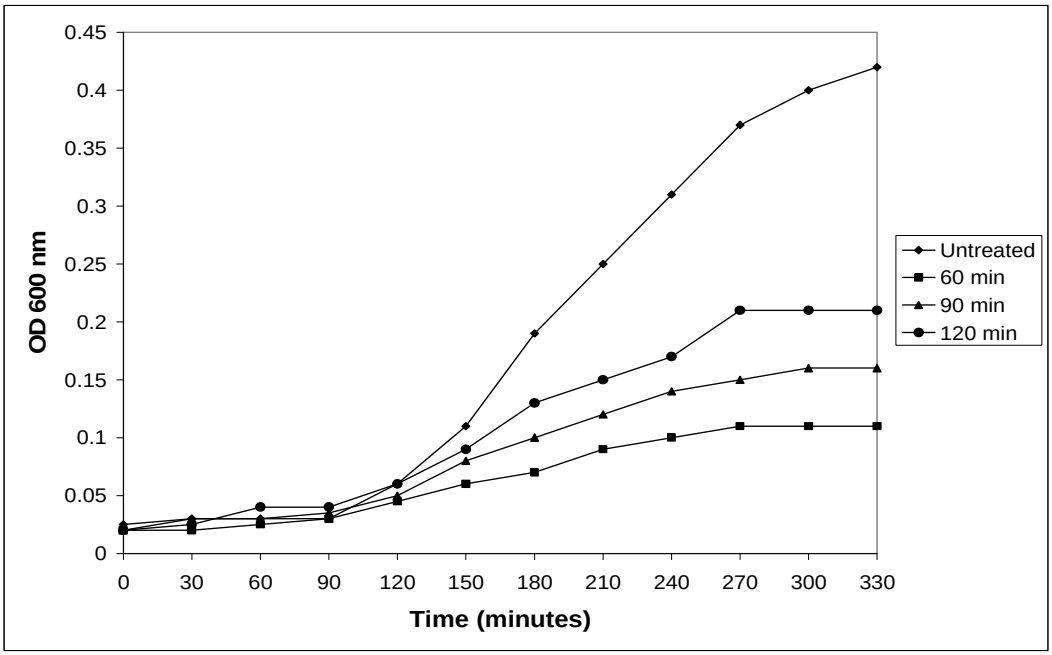

Figure 21. Effect of 1 mM paraquat on growth rate of ER2566 cultured in NB. Untreated and treated cultures were grown in parallel in 4 mL NB. Separate treated cultures received 40 μL of 1 mM paraquat 60, 90, and 120 minutes following inoculation and untreated culture received 40 μL of sterile H_2O. Optical density measurements were taken at 30 minute intervals at a wavelength of 600 nm with a Spec 20+.

Effect of Paraquat on Growth Rate of ATCC 4157

The effect of 0.5 mM paraquat on ATCC 4157 cells was investigated for cells cultured in the three growth media tested for ER2566, Luria-Bertani broth, double strength Luria-Bertani broth, and nutrient broth. In contrast to results obtained for ER2566, a bacteriostatic effect was observed for cells cultured in LB with 0.5 mM paraquat at all times tested (Figure 22). When added 30 minutes following inoculation, growth rate was greatly affected, being reduced by greater than 50%, with a slight decrease in optical density measurements occurring 3 hours after addition of paraquat. Addition of paraquat 60 minutes following inoculation produced the desired reduction in growth rate of around 50% in this medium.

In contrast to ER2566, the bacteriostatic effect of paraquat was greater in 2XLB than LB for ATCC 4157 (Figure 23). Culture growth rate was reduced by 50% following addition of 0.5 mM paraquat 90 minutes after inoculation, 30 minutes later than observed for cells cultured in LB. In addition, paraquat added 60 minutes following inoculation resulted in a decrease in growth almost as much as observed when added at 30 minutes, with a decrease in optical density observed for both 3 hours after paraquat addition. Similar to ER2566, the greatest bacteriostatic effect of paraquat was observed on cells cultured in nutrient broth (Figure 24). In this medium, the reduction in growth rate occurring for the culture treated 120 minutes following inoculation was greater than that observed for cells treated at the same time in LB and 2XLB.

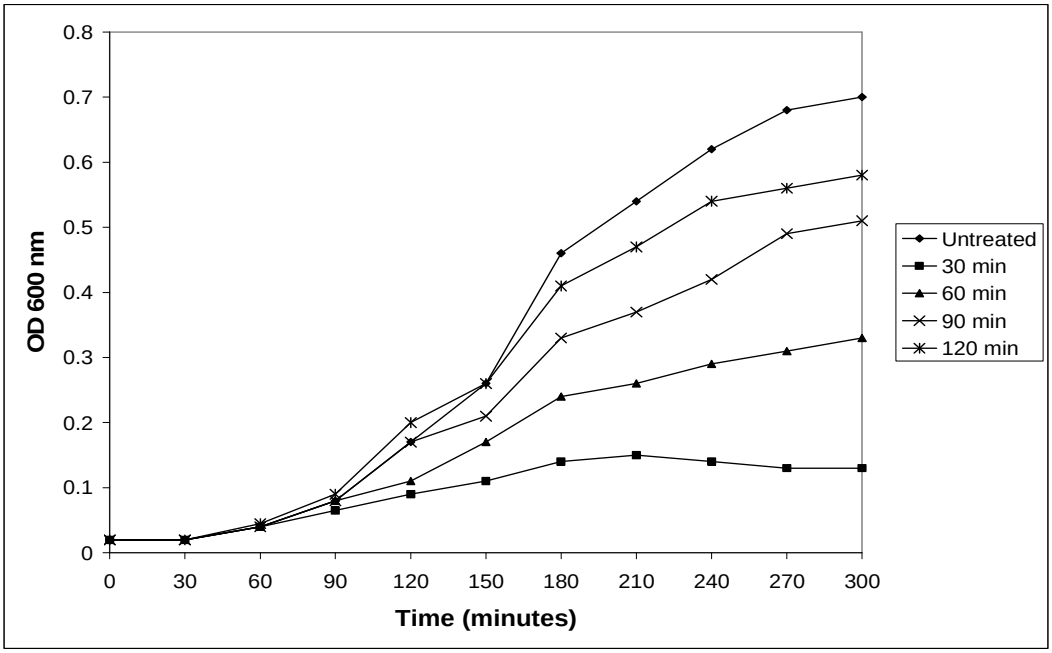

Figure 22. Effect of 0.5 mM paraquat on growth rate of ATCC 4157 cultured in LB. Untreated and treated cultures were grown in parallel in 4 mL LB. Separate treated cultures received 40 µL of 0.5 mM paraquat 30, 60, 90, and 120 minutes following inoculation and untreated culture received 40 µL of sterile H_2O. Optical density measurements were taken at 30 minute intervals at a wavelength of 600 nm with a Spec 20+.

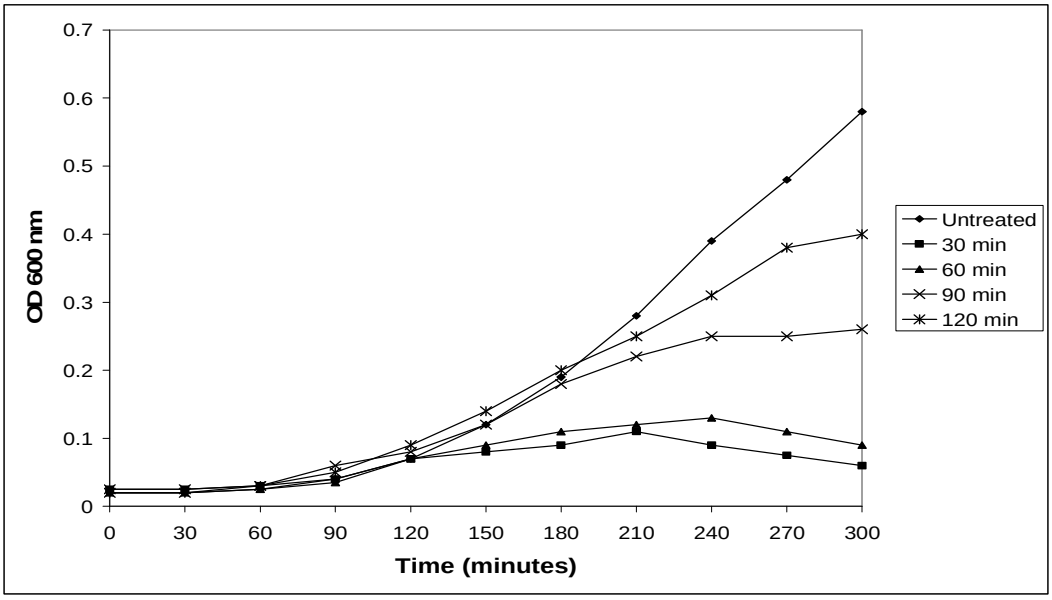

Figure 23. Effect of 0.5 mM paraquat on growth rate of ATCC 4157 cultured in 2XLB. Untreated and treated cultures were grown in parallel in 4 mL 2XLB. Separate treated cultures received 40 µL of 0.5 mM paraquat 30, 60, 90, and 120 minutes following inoculation and untreated culture received 40 µL of sterile H_2O. Optical density measurements were taken at 30 minute intervals at a wavelength of 600 nm with a Spec 20+.

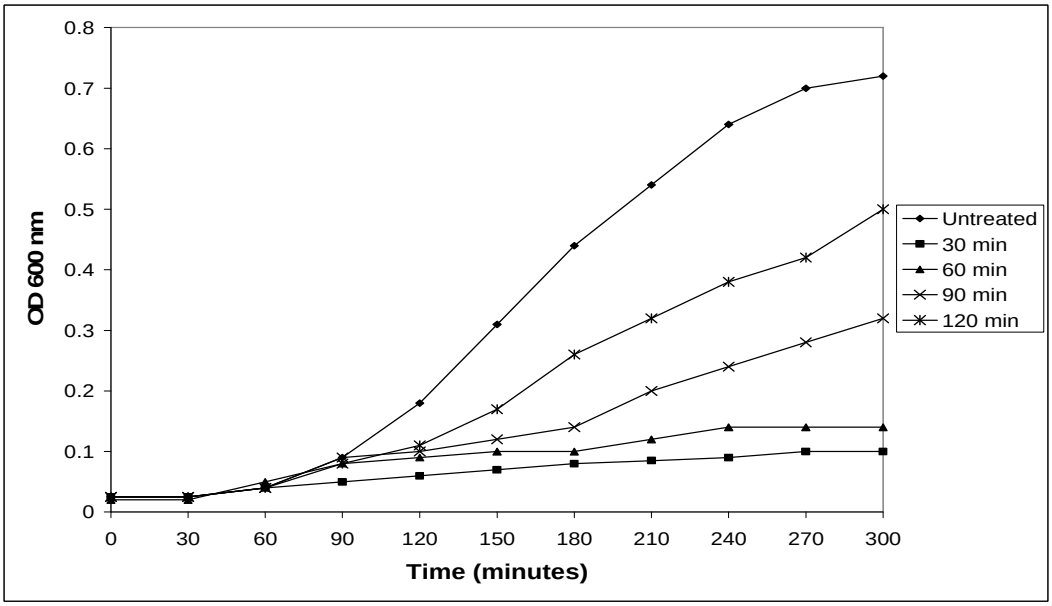

Figure 24. Effect of 0.5 mM paraquat on growth rate of ATCC 4157 cultured in NB. Untreated and treated cultures were grown in parallel in 4 mL NB. Separate treated cultures received 40 µL of 0.5 mM paraquat 30, 60, 90, and 120 minutes following inoculation and untreated culture received 40 µL of sterile H_2O. Optical density measurements were taken at 30 minute intervals at a wavelength of 600 nm with a Spec 20+.

3. LIVE/DEAD BACLIGHT BACTERIAL VIABILITY KIT

Calibration of SYTO9 and Propidium Iodide for ER2566

Based on results previously obtained in the lab, SYTO9 concentrations below 2 μM were selected for further calibration of the dye for ER2566. The manufacturer's instructions were followed for the kit, with cell density adjusted as recommended to 0.06 at 670 nm, which the protocol states gives a cell concentration of approximately 2×10^8 cells/mL. According to the conversion factors obtained for log phase cells with the spread-plate method and hemacytometer, this optical density corresponds to 6×10^6 CFUs/mL and 2.4×10^6 cells/mL, respectively. As shown in Figure 25, green fluorescent intensity measured at 520 nm peaked at a SYTO9 concentration of 1.25 μM, indicating saturation of the cell suspension with this concentration.

Following calibration of SYTO9, propidium iodide was calibrated using a range of live to dead cell ratios (Figure 26). Both live and dead cell suspensions were adjusted to OD_{670} 0.06 as recommended by the manufacturer. With the concentration of SYTO9 held constant, a range of propidium iodide concentrations between 1 and 5 μM was tested, with each concentration tested for each live/dead ratio. Again, this concentration range was narrowed based on data previously obtained in the lab using a wider range. The data were analyzed using a plot of green/red fluorescence ratio versus the percentage of live bacteria. With the highest coefficient of determination, 4 μM was chosen as the optimal concentration of propidium iodide for ER2566.

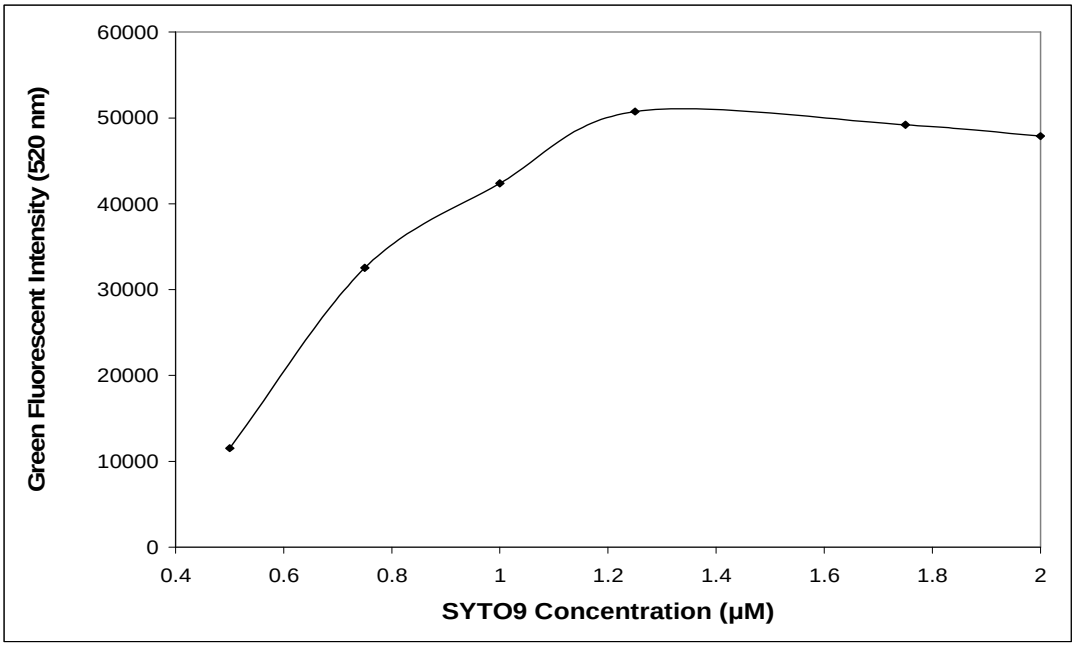

Figure 25. Calibration of SYTO9 for ER2566. Cells in late log phase were harvested by centrifugation and adjusted to OD_{670} 0.06 with a Spec 20+. Cells were incubated with dye in a Costar 3915 96-well microplate for 15 minutes and fluorescence measurements recorded at 520 nm with a POLARstar OPTIMA fluorescence microplate reader.

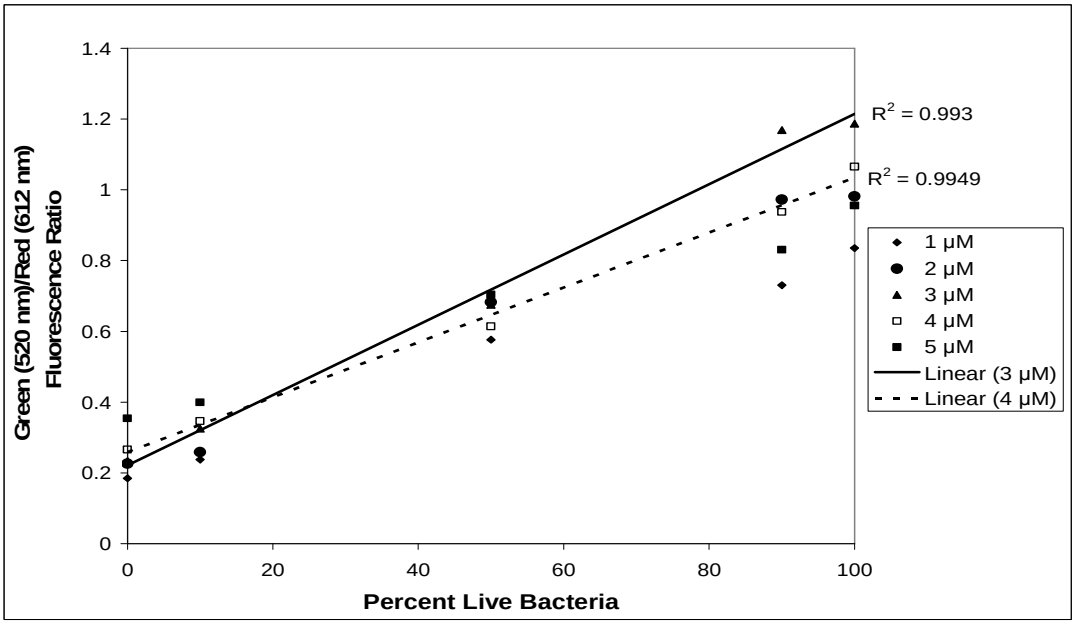

Figure 26. Propidium Iodide Calibration for ER2566. Five different live/dead cell ratios were stained with a mixture of SYTO9 and PI and fluorescence intensity measured at the optimum wavelength of each dye. The green/red fluorescence ratio was calculated for each live/dead ratio and plotted against the percentage of live bacteria. Linear regression was performed and the coefficient of determination calculated for each PI concentration (only 2 highest R^2 values shown).

Calibration of SYTO9 and Propidium Iodide for ATCC 4157

Due to potential differences between membrane permeability of the two *E. coli* strains, SYTO9 and propidium iodide were also calibrated for ATCC 4157. As with ER2566, when calibrating each dye, cell suspensions were adjusted to OD_{670} 0.06 as recommended by the manufacturer. Initially the same range of SYTO9 concentrations tested for ER2566 was tested for ATCC 4157 (0.5-2 μM). However, the saturation curve did not appear to peak but was still increasing at the highest dye concentration tested (data not shown). Therefore, a wider range of SYTO9 concentrations (2-16 μM) was tested. As shown in Figure 27, fluorescent intensity did not peak until a SYTO9 concentration of 12 μM, with quenching occurring at 16 μM. As shown in Figure 28, the optimal concentration of propidium iodide was determined to be 100 μM, a concentration 25X that required for ER2566.

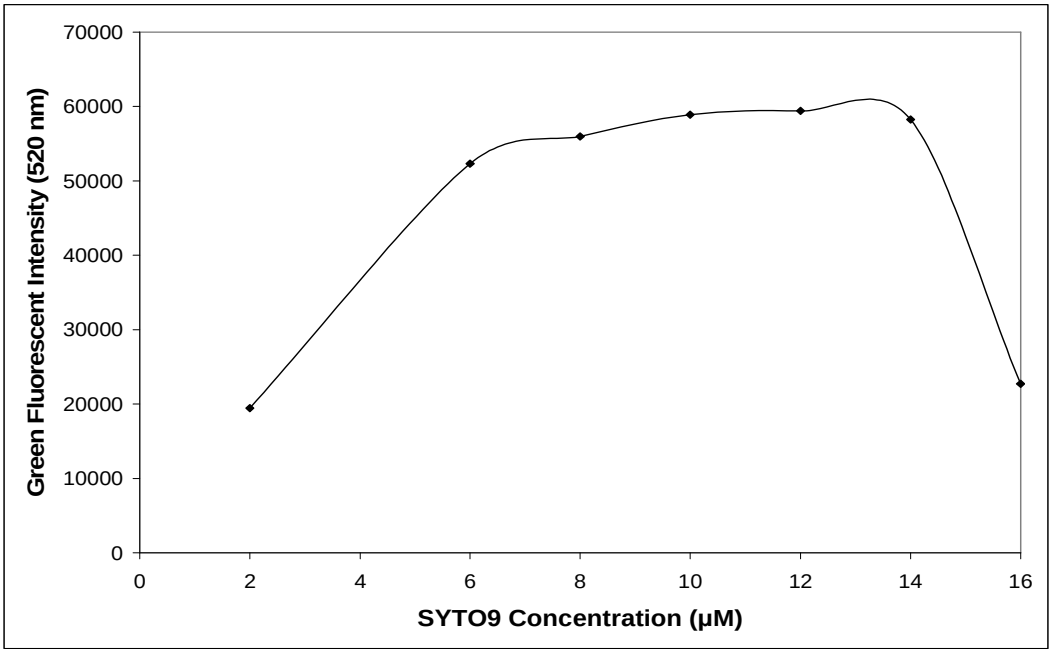

Figure 27. SYTO9 Calibration for ATCC 4157. Cells in late log phase were harvested by centrifugation and adjusted to OD_{670} 0.06 with a Spec 20+. Cells were incubated with dye in a Costar 3915 96-well microplate for 15 minutes and fluorescence measurements recorded at 520 nm with a POLARstar OPTIMA fluorescence microplate reader.

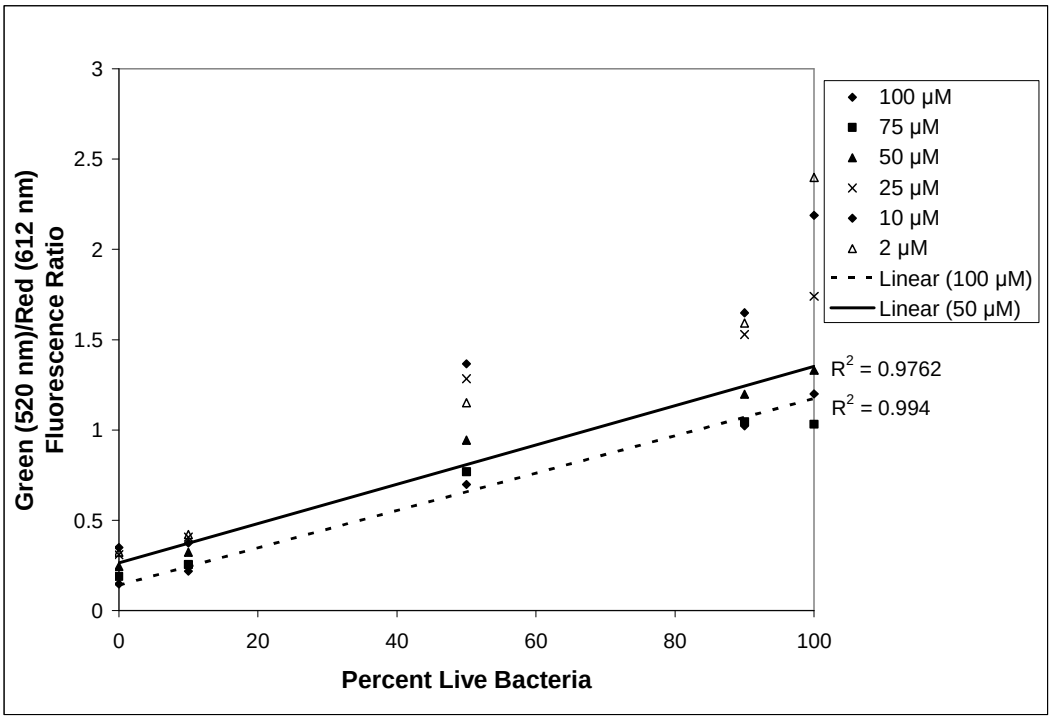

Figure 28. Propidium Iodide Calibration for ATCC 4157. Five different live/dead cell ratios were stained with a mixture of SYTO9 and PI and fluorescence intensity measured at the optimum wavelength of each dye. The green/red fluorescence ratio was calculated for each live/dead ratio and plotted against the percentage of live bacteria. Linear regression was performed and the coefficient of determination calculated for each PI concentration (only 2 highest R^2 values shown).

Effect of High Dye Concentrations on Fluorescence Measurements

The requirement of such high dye concentrations meant that fewer assays could be performed with the BacLight kit, making it a more costly means of determining cell viability for ATCC 4157 than for ER2566. In addition, high dye concentrations could interfere with fluorescence measurements, a phenomenon known as the inner filter effect. The proportionality between concentration and fluorescence intensity only occurs for optical densities less than 0.05 as shown in Figure 29. Therefore, it seemed unlikely that the kit could be used for this strain and that cell viability would have to be assessed using an alternative method. Tests for the inner filter effect confirmed that at these high dye

concentrations, the kit could not be used. To test for inner filter effects, absorbance at the excitation and emission wavelengths of the two dyes was tested for three proportions of live/dead cells, with separate measurements taken for the cells alone (cells with buffer), each dye alone (dye with buffer), cells stained with SYTO9 only, cells stained with PI only, cells stained with a dye mixture, and dye mixture alone (SYTO9 + PI with buffer). As shown in Table 4, all optical density measurements exceeded 0.05 at each wavelength.

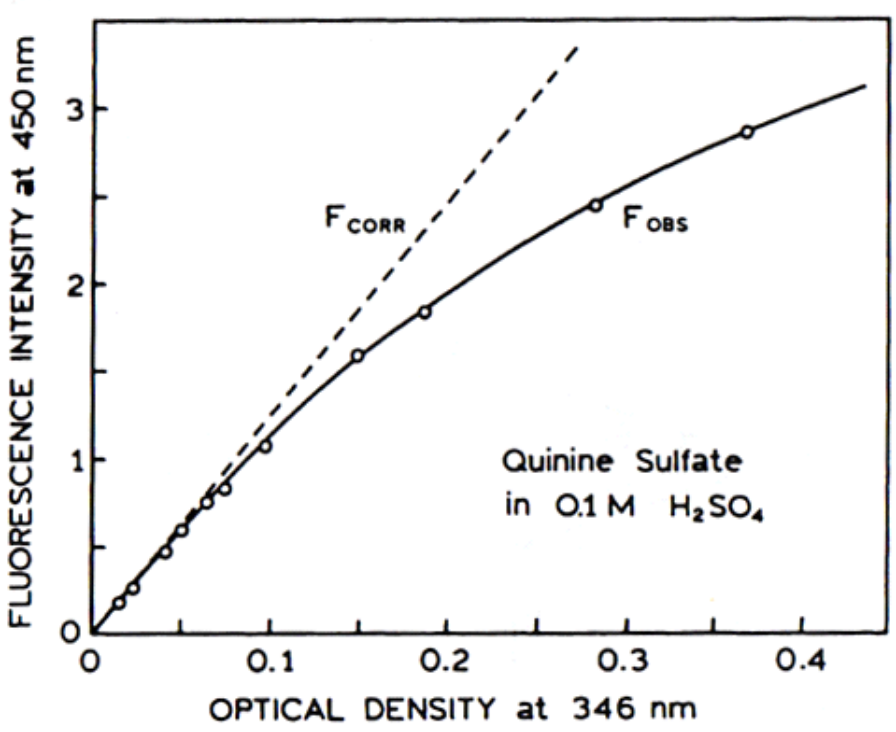

Figure 29. Relationship between optical density and fluorescence intensity, shown using quinine sulfate. The dashed line shows fluorescence intensity corrected for the inner filter effect for each optical density, while the solid line shows actual fluorescence intensity obtained at each optical density (from Lakowicz 2006).

Table 4. Optical density test for inner filter effects for ATCC 4157. Cells were prepared for staining according the protocol for the BacLight kit with OD_{670} adjusted to 0.06 with the Spec 20+. The concentration of SYTO9 tested was 12 μM and the concentration of PI tested was 100 μM. Optical density measurements were taken at the excitation and emission wavelengths for each dye with the SpectraMax 190 microplate spectrophotometer.

Optical Density at Emission and Excitation Wavelengths									
λ (nm)	**0% Live (cells only)**	**50% Live (cells only)**	**100% Live (cells only)**	**SYTO9 (w/o cells)**	**PI (w/o cells)**	**SYTO9 & PI (w/o cells)**	**SYTO9 w/ cells**	**PI w/ cells**	**SYTO9 & PI w/ cells**
485	0.121	0.110	0.111	0.467	0.677	1.103	0.523	0.770	1.106
520	0.116	0.106	0.107	0.076	0.550	0.568	0.156	0.624	0.617
612	0.108	0.099	0.100	0.070	0.082	0.087	0.114	0.129	0.131

Effect of cell density conversion factor on calibration of BacLight dyes for ATCC 4157

According to the conversion factor between optical density measurements and cell number obtained for ATCC 4157 (Tables 2 & 3), adjusting cell suspensions as recommended by the manufacturer to OD_{670} 0.06 resulted in a cell concentration of 6 x 10^6 CFUs/mL and 1.8 x 10^5 cells/mL. Using the CFUs/mL conversion, an OD_{670} of 0.2 would correspond to the manufacturer's recommended cell concentration of 2 x 10^8 cells/mL. By adjusting the cell suspension to OD_{670} 0.2 prior to staining, the optimal SYTO9 concentration was determined to be 6 μM (Figure 30) and the optimal propidium iodide concentration was determined to be 20 μM (Figure 31) for ATCC 4157.

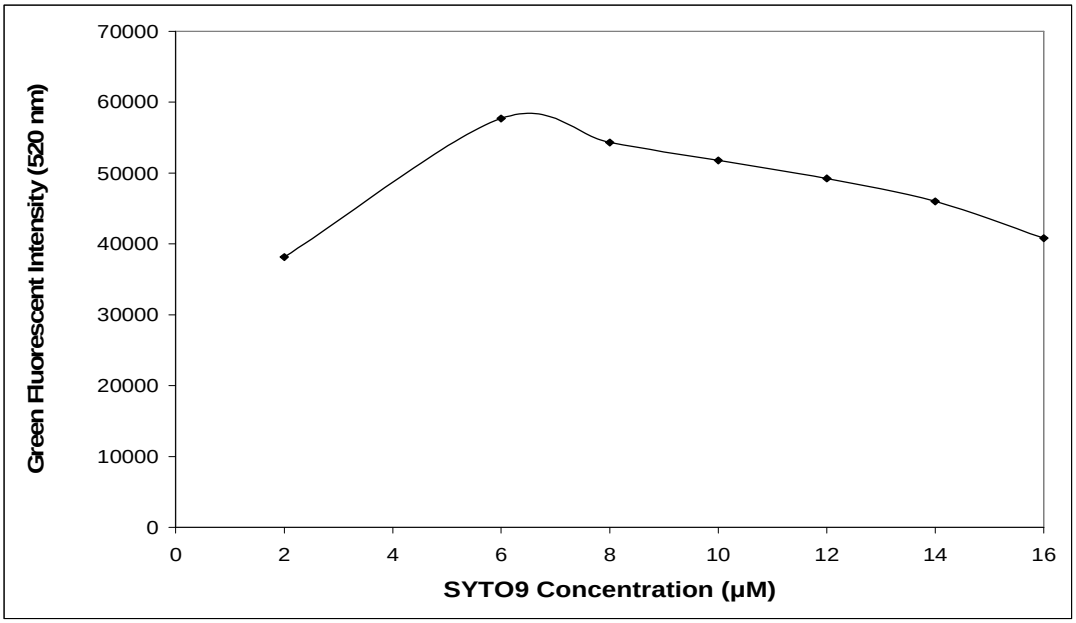

Figure 30. SYTO9 Saturation for ATCC 4157 with OD_{670} 0.2. Cells in late log phase were harvested by centrifugation and adjusted to OD_{670} 0.2 with a Spec 20+. Cells were incubated with dye in a Costar 3915 96-well microplate for 15 minutes and fluorescence measurements recorded at 520 nm with a POLARstar OPTIMA fluorescence microplate reader.

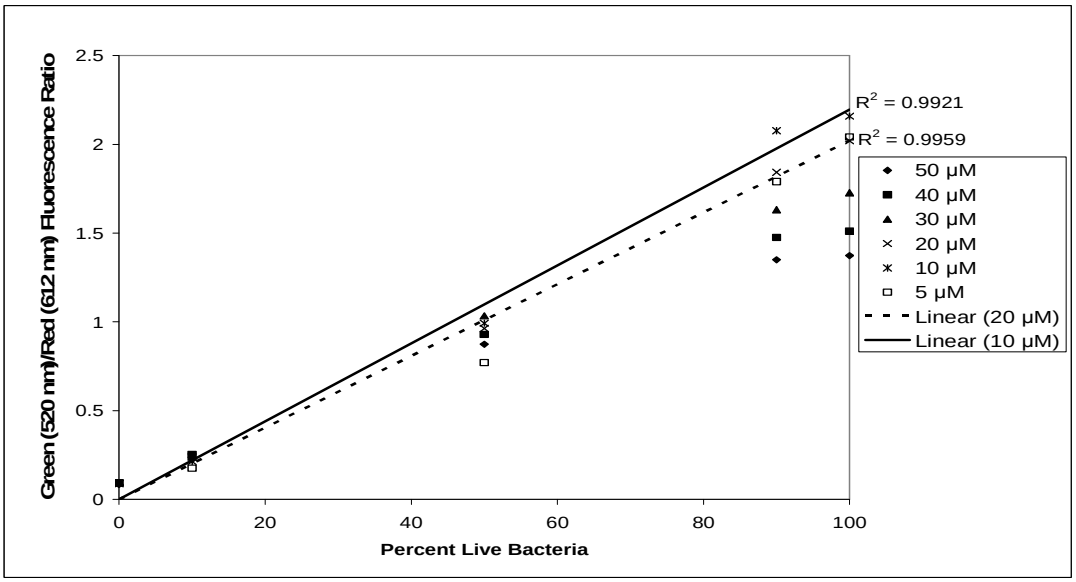

Figure 31. Propidium Iodide Calibration for ATCC 4157 with OD_{670} 0.2. Five different live/dead cell ratios were stained with a mixture of SYTO9 and PI and fluorescence intensity measured at the optimum wavelength of each dye. The green/red fluorescence ratio was calculated for each live/dead ratio and plotted against the percentage of live bacteria. Linear regression was performed and the coefficient of determination calculated for each PI concentration (only 2 highest R^2 values shown).

Assessment of Automatic Pipetter on Fluorescence Measurements

When transferring cell suspension and dye mixture to the 96-well microplate, an automatic pipetter (Impact^2) was used to enable faster loading and to increase accuracy. To ensure that during loading cells were not settling in the pipet tip resulting in different cell concentrations in each well, fluorescence measurements were compared between an automatic pipetter and a manual pipetter using the nucleic acid stain DAPI. As shown in Table 5, fluorescence intensity fluctuated with each pipetter, with fluctuations being greater for the automatic pipetter for the first 6 wells. However, a similar pattern was found for both pipetters for the last 4 wells. The average fluorescent intensity and standard deviations for the manual and automatic pipetters were calculated to be 50893 ± 6671 and 52097 ± 9030, respectively.

Table 5. Effect of Pipetter Type on Fluorescence Measurements. ER2566 cells were transferred into a Costar 3915 96-well microplate, one row transferred with an automatic pipetter and another row transferred with a manual pipetter. Cells were incubated with DAPI overnight and fluorescent intensity at 460 nm recorded with a POLARstar OPTIMA fluorescence microplate reader.

	Blue Fluorescent Intensity (460 nm)	
Well Number	**Manual Pipetter**	**Automatic Pipetter**
1	48543	41695
2	48309	47212
3	52377	59754
4	48273	52182
5	49039	55849
6	50575	51036
7	57971	57133
8	52722	53724
9	56495	53768
10	44629	48612
Average (± standard deviation)	**50893 ± 6671**	**52097 ± 9030**

4. SOD INHIBITION WITH DIETHYLDITHIOCARBAMATE (DDC)

DDC Concentration Determination

The growth rate of ER2566 was completely inhibited when treated immediately following inoculation with DDC at concentrations of 0.1, 0.2, 0.4, and 1 mM (data not shown). Based on these results, micromolar concentrations were tested, with the results of treatment with 20 μM DDC shown in Figure 32. No increase in optical density occurred for the first hour following treatment, with an increase in optical density of only 0.01 occurring between 60 minutes and 120 minutes. However, growth resumed after two hours, with optical density measurements doubling as usual for log phase growth.

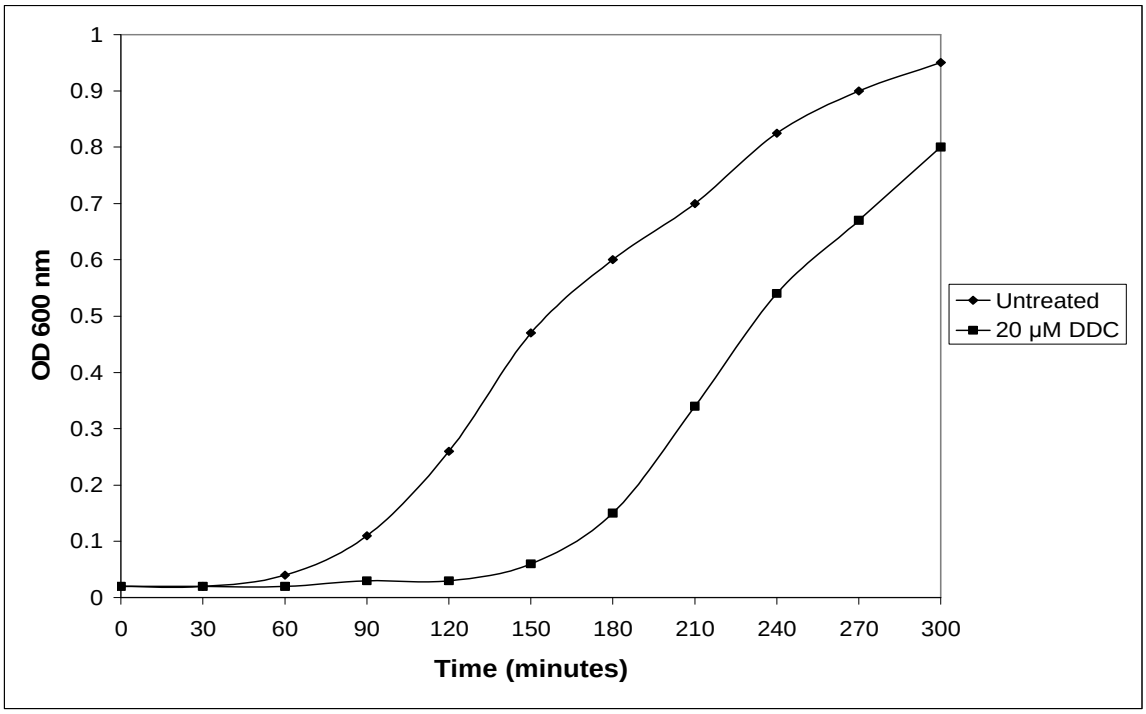

Figure 32. Effect of 20 μM DDC on Growth Rate of ER2566. Untreated and treated cultures were grown in parallel in 4 mL NB. Treated culture received 40 μL of 20 μM DDC following inoculation and untreated culture received 40 μL of sterile H_2O. Optical density measurements were taken at 30 minute intervals at a wavelength of 600 nm with a Spec 20+.

DDC and Paraquat Combination Treatment

The effect of simultaneous DDC and paraquat treatment on the cell was assessed using ER2566 cultured in nutrient broth. Cells were treated with 1 mM paraquat, since this was the concentration shown to reduce culture growth rate by 50%, and 20 μM DDC and cultured in parallel with untreated cells and cells receiving treatment with only paraquat or DDC. As shown in Figure 33, the growth rate of the culture treated with both 1 mM paraquat and 20 μM DDC was less affected than the growth rate of the cultures receiving only one treatment. However, growth was reduced compared to the untreated culture 90 minutes after paraquat addition. In addition, optical density measurements declined at 210 minutes following addition of paraquat, while the growth rate of the two cultures receiving only one treatment began to level off near the end of the measurement period.

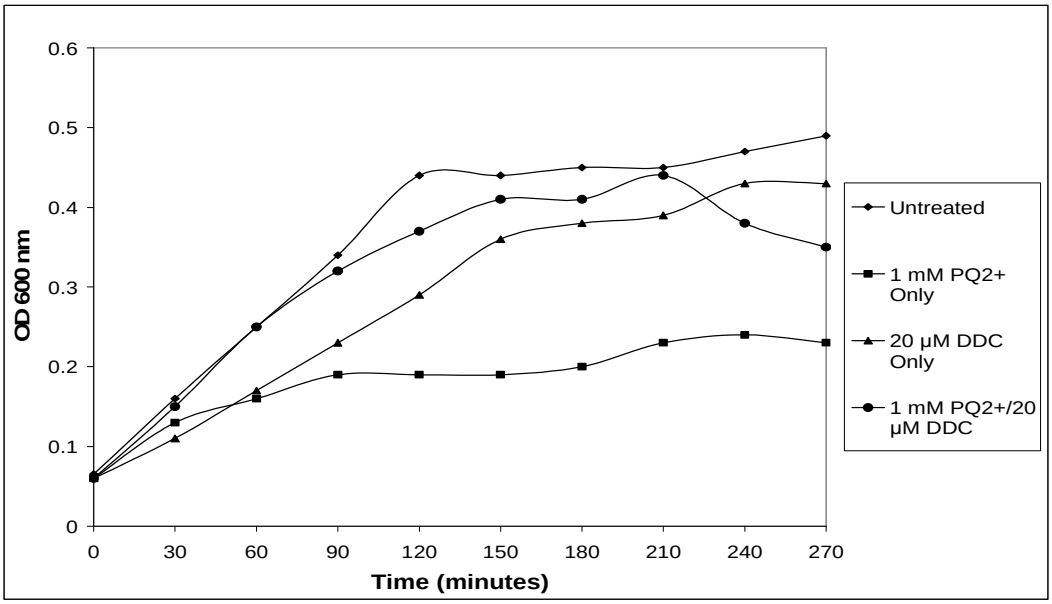

Figure 33. ER2566 treated with both 1 mM paraquat and 20 μM DDC. Untreated and treated cultures were grown in parallel in 4 mL NB. DDC was added to treated cultures following inoculation with overnight culture. Paraquat was added to treated cultures 120 minutes following inoculation with overnight culture. OD measurements were taken at 30 minute intervals after PQ^{2+} addition at a wavelength of 600 nm with Spec 20+.

5. XANTHINE/XANTHINE OXIDASE ASSAY

Cell viability following xanthine/xanthine oxidase treatment in PPB, pH 6.5

Under the same treatment conditions, a reduction in cell viability was only observed for ER2566 (Figures 34 and 35). For ER2566, the biggest decrease in cell viability occurred within the first 30 minutes of treatment, with numbers leveling off for the remaining treatment period. In addition, there was a slight decrease in CFUs for untreated cells during the 2 hour incubation period. In contrast, a similar trend was observed for CFU counts for both untreated and treated ATCC 4157 cultures. A decrease in the number of CFUs for both strains was observed at 90 minutes.

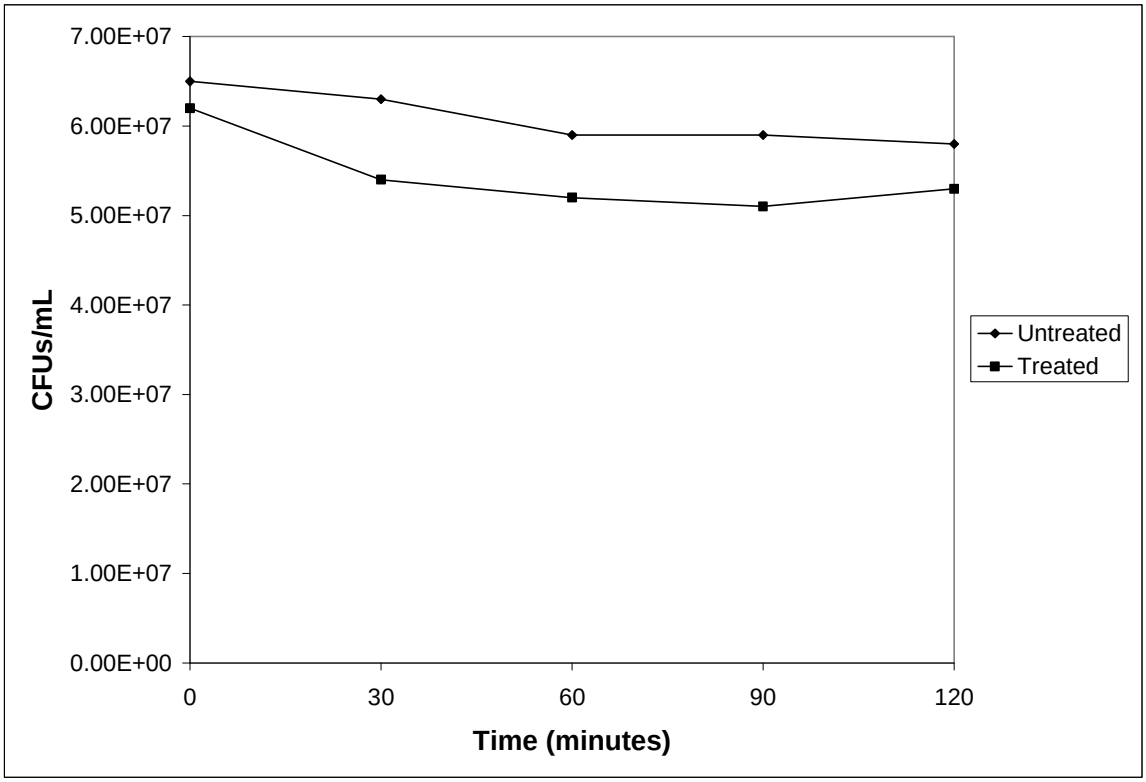

Figure 34. Effect of xanthine/xanthine oxidase treatment on viability of ER2566 at pH 6.5. Cells were harvested in stationary phase and resuspended in PPB adjusted to a pH of 6.5. Both untreated and treated cells received 1 mL xanthine solution (0.05 mM). Untreated cells received 100 μL H_2O while treated cells received 100 μL xanthine oxidase (0.02 units). Cell viability was assessed using the spread-plate method.

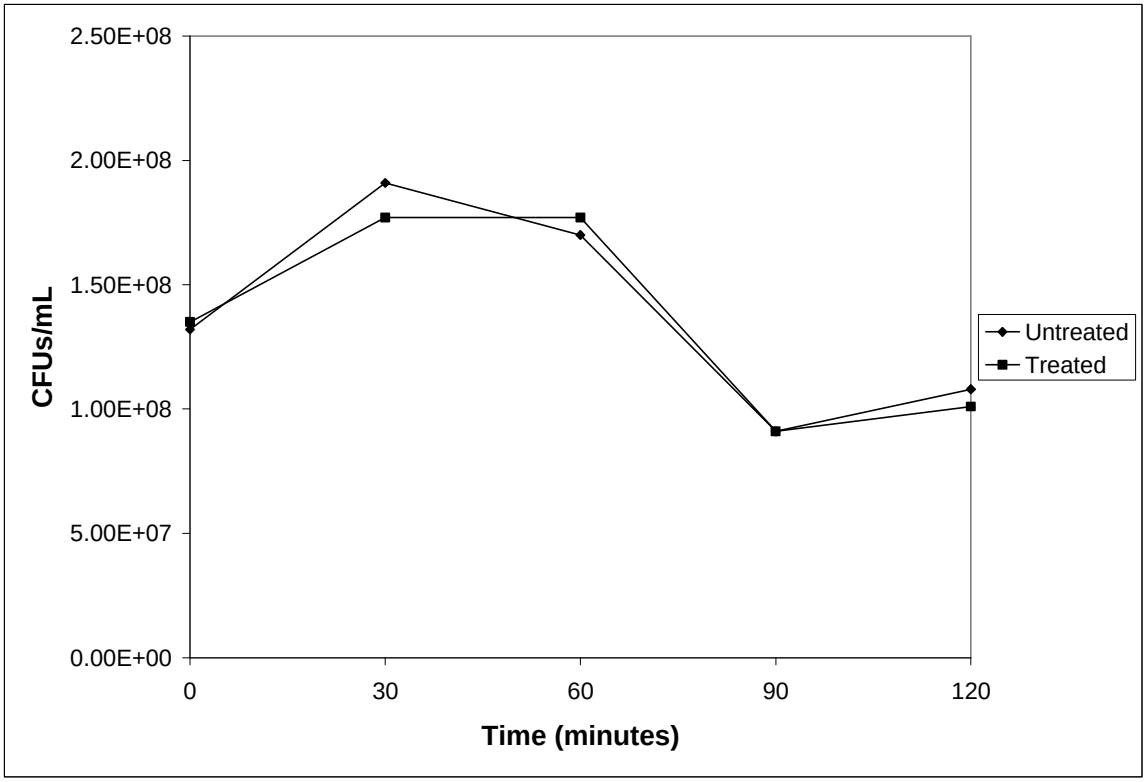

Figure 35. Effect of xanthine/xanthine oxidase treatment on viability of ATCC 4157 at pH 6.5. Cells were harvested in stationary phase and resuspended in potassium phosphate buffer adjusted to a pH of 6.5. Both untreated and treated cells received 1 mL xanthine solution (0.05 mM). Untreated cells received 100 μL H_2O while treated cells received 100 μL xanthine oxidase (0.02 units). Cell viability was assessed using the spread-plate method.

Evalulation of methods to assess cell viability following treatment with xanthine/xanthine oxidase at pH 7.5

To determine the best method to assess cell viability following xanthine/xanthine oxidase treatment, cell viability was determined using the spread-plate method and the BacLight kit for ER2566 treated cells. To examine the effects of pH on toxicity, the pH of the buffer was increased to 7.5. In contrast to results obtained counting colony-forming units at a pH 6.5, no difference was observed between untreated cells and treated cells for the first hour of treatment (Figure 36). However, a decrease in CFUs was observed after 90 and 120 minutes of treatment. In contrast to the spread-plate method,

the BacLight kit did detect a decrease in cell viability at the beginning of treatment. However, at 60 minutes, there was an increase in the percentage of cells reported live (Figure 37). At 90 and 120 minutes of treatment, cell viability decreased as observed with the spread-plate method, with percentage of live cells reduced from 90.5% to 73.6% at 90 minutes.

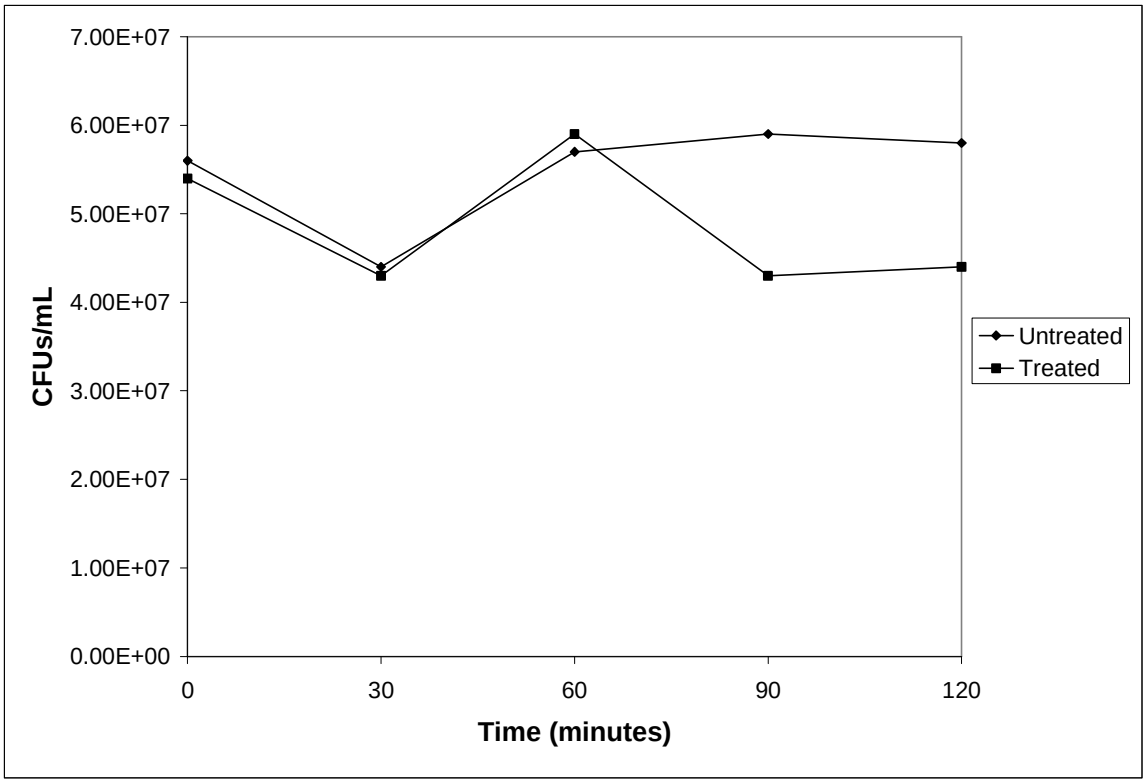

Figure 36. Assessment of xanthine/xanthine oxidase treatment on viability of ER2566 using the spread-plate method. Cells were harvested in stationary phase and resuspended in potassium phosphate buffer adjusted to a pH of 7.5. Both untreated and treated cells received 1 mL xanthine solution (0.05 mM). Untreated cells received 100 μL H_2O while treated cells received 100 μL xanthine oxidase (0.02 units).

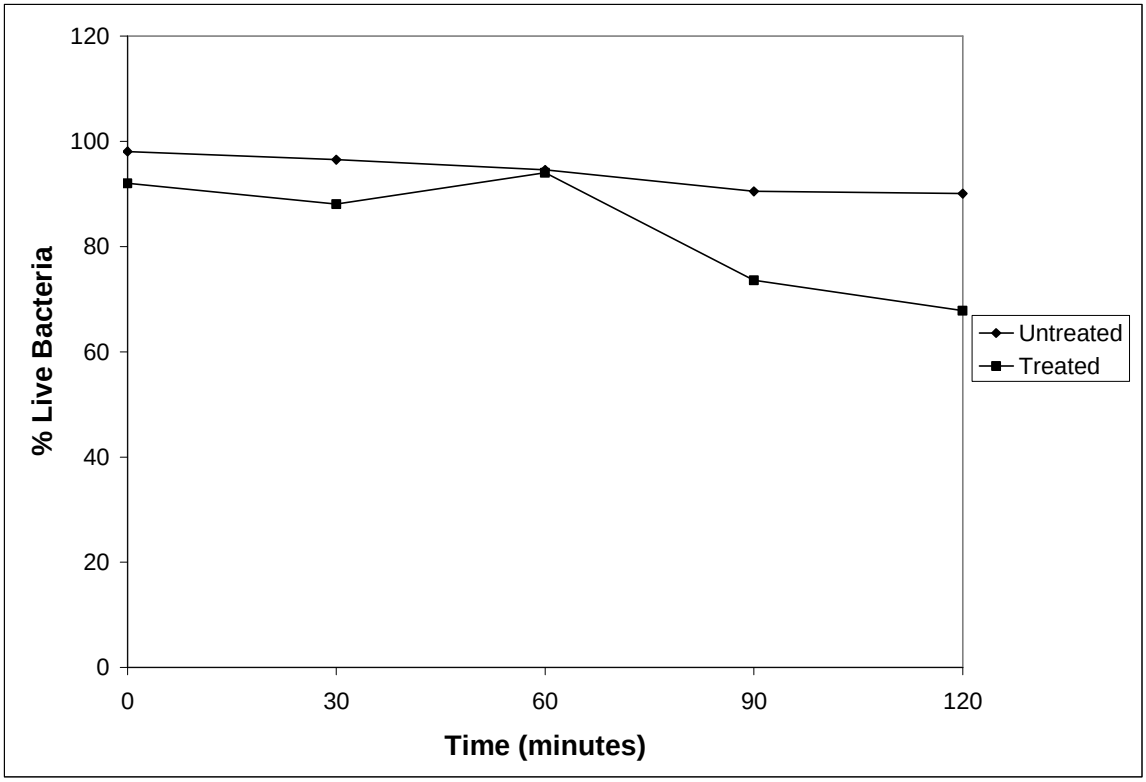

Figure 37. Assessment of xanthine/xanthine oxidase treatment on viability of ER2566 using the BacLight kit. Cells were harvested in stationary phase and resuspended in potassium phosphate buffer (pH 7.5) to OD_{670} 0.06. Both untreated and treated cells received 1 mL xanthine solution (0.05 mM). Untreated cells received 100 μL H_2O while treated cells received 100 μL xanthine oxidase (0.02 units).

DISCUSSION

Relationship between optical density measurements and cell concentration

As previously mentioned, different strains of *E. coli* can scatter light differently causing each to have a different relationship between optical density and cell concentration. This difference in light scattering is due in part to the diversity in lipopolysaccharides (LPS) present on the outer membrane and extending into the surrounding medium (Raetz and Whitfield 2002). LPS are composed of three parts: lipid a, core oligosaccharide, and O-antigen. Differences between LPS of bacterial strains are primarily due to differences in the composition of the O-antigen. Although no information is available regarding the lipopolysaccharides of ER2566, the O-antigen is usually absent from laboratory strains, a condition referred to as a rough LPS (Raetz and Whitfield 2002). Strain ATCC 4157 was specifically chosen due to the presence of the full-length O-antigen rendering its LPS smooth. This selection was necessary for future neutrophil assays, as the O-antigen protects against complement-mediated killing by serum. The bacterium may then be opsonized with serum, which enables phagocytosis by professional phagocytes (Papp-Szabo et al. 1993). Thus the finding that each strain had a different relationship between optical density measurements and cell counts obtained with both CFU counts and total cell counts is not surprising. However, this information is essential when using optical density measurements as an indicator of the effectiveness of a particular experimental treatment on a culture. As the data show, at a particular OD_{670} during log phase, a suspension of ER2566 is much more concentrated than ATCC 4157. In contrast, for stationary phase cells the reverse is true, with a

suspension of ATCC 4157 being much more concentrated than ER2566 at a particular OD_{670}. This difference is a factor that needs to be taken into consideration when comparing experimental data between the two strains.

Assessing paraquat toxicity with cell density measurements

The decrease in optical density observed for cultures treated with 0.5 and 0.75 mM paraquat highlights the drawback of using optical density measurements as an indication of cell growth. As discussed earlier, optical density measurements do not allow discrimination between viable cells and non-viable cells since both are able to scatter light. Therefore, a decrease in optical density cannot be interpreted as cell death. In addition, previous studies of paraquat toxicity on *E. coli* have reported that paraquat concentrations exceeding 100 μM are required for lethality, with concentrations less than 10 μM having a bacteriostatic effect (Kitzler and Fridovich 1986).

The viability of cells was confirmed with CFU counts prepared alongside optical density measurements immediately before, during, and after the decline observed at these paraquat concentrations (data not shown). Instead of the number of CFUs decreasing during the decline, a plateau occurred.

The disparity between growth curves and what is actually happening to a culture has been previously reported with *E. coli* cells treated with antibiotics. In these studies, optical density measurements increased immediately following antibiotic treatment indicating culture growth; however, CFU counts remained steady during this treatment period and the increase in OD was attributed to the formation of cells with damaged walls (Yourassowsky et al. 1985). To date, none of the researchers utilizing paraquat to

generate superoxide have reported a decrease in optical density while monitoring the rate of growth. The biological mechanisms behind this phenomenon remain unknown.

Effect of culture medium on paraquat toxicity

The relationship between growth medium and paraquat toxicity has been previously investigated with a variety of medium types including trypticase/soy/yeast (TSY), nutrient broth, glucose minimal medium, and Vogel-Bonner (VB) medium (Kitzler and Fridovich 1986 a & b, Hassan and Fridovich 1978). These investigators report that yeast extract and salts provide protection against the toxicity of paraquat. The protection afforded to cells by yeast extract has been attributed to the nutritional supplementation it provides. Yeast extract provides carbohydrates, vitamins, micronutrients and proteins that enable the cell to synthesize enzymes necessary for the production of branched-chain amino acids (valine, leucine, isoleucine) and pyridine coenzymes to replace those that have been damaged by superoxide. The protection against paraquat toxicity provided by yeast extract is substantial. A previous study found that cells grown in medium supplemented with yeast extract and treated with a lethal concentration of paraquat (100 μM) had a reduction of 31% in growth, while growth of cells cultured in yeast extract-free medium was completely eliminated (Kitzler and Fridovich 1986a). In addition to replacement of these enzymes, yeast extract has also been shown to enable the cell to increase biosynthesis of manganese superoxide dismutase during oxidative stress generated by paraquat (Hassan and Fridovich 1978). These investigators reported that the concentration of MnSOD in paraquat treated cells

grown in medium supplemented with yeast extract was 7X that of treated cells cultured in yeast-extract free medium.

In contrast to the protection provided by yeast extract, the protection provided by salt has been attributed to inhibition of paraquat uptake into the cell. Paraquat is actively taken up by cells against a concentration gradient and is accumulated within the cell (Kao and Hassan 1985). Although the salts of both monovalent cations and divalent cations have been shown to inhibit paraquat uptake, the salts of divalent cations provided greater protection against paraquat toxicity, most likely because paraquat is also a dication (Kitzler and Fridovich 1986b). However, these investigators found no differences between CFU counts of untreated cells and cells treated with 1 mM paraquat in nutrient broth supplemented with 100 mM NaCl, indicating that full protection was provided by the monocation salt.

The effect of culture medium on paraquat toxicity was most pronounced in ER2566. The increased susceptibility of these cells to paraquat when cultured in nutrient broth compared to Luria-Bertani broth could be due to differences in media ingredients, as nutrient broth does not contain yeast extract. Luria-Bertani broth contains NaCl at a concentration of 86 mM, a concentration comparable to that used in the above mentioned experiment by Kitzler and Fridovich, while double-strength Luria-Bertani broth contains a concentration of 172 mM NaCl. The possibility of ingredient influence is further supported by the failure of paraquat to reduce culture growth rate in double strength Luria-Bertani broth even when present at twice the concentration of that tested in LB, 1 mM compared to 0.5 mM. While a clear difference was observed between media types and paraquat toxicity for ER2566, the same trends were not observed for the clinical

isolate, ATCC 4157. However, the strain was clearly more susceptible to paraquat in nutrient broth compared to LB and 2XLB. At this time, it can only be speculated that the greater susceptibility of ATCC 4157 to paraquat in LB and 2XLB compared to ER2566 is due to differences in membrane permeability. With ER2566 being a lab strain and ATCC 4157 a clinical isolate, it is probable that each has evolved different adaptations to survive in their optimal environments, which could greatly impact their ability to tolerate oxidative stress.

Effect of SOD inhibition during oxidative stress on growth rate of ER2566

The ability of a CuZnSOD inhibitor to decrease log phase growth highlights how little is understood about the role of this SOD within the cell. Although DDC is a chelator of both copper and zinc, its ability to inhibit CuZnSODs has been attributed to the removal of copper from the active site. Thus, given the present understanding that *sodC* is not expressed until stationary phase, the mechanism by which DDC affects cell growth must be unrelated to its inhibition of CuZnSODs. Although merely speculative given the lack of experimental evidence, it is possible that this reduction in growth occurred due to inhibition of metalloproteinases by DDC, preventing recycling of amino acids needed in the biosynthesis of proteins. Metal chelation by DDC was indicated in a recent study as the mechanism by which DDC was able to kill drug-resistant *Mycobacterium tuberculosis* (Byrne et al. 2007). A previous study investigating the effect of DDC on the growth rate of *E. coli* found that at a concentration of 50 μM, DDC was able to inhibit aerobic growth of *E. coli* to an extent comparable to that obtained for ER2566 (Benov and Fridovich 1996). These investigators were unable to explain the

mechanism by which DDC exerted it effects, but speculated that CuZnSODs may not be isolated completely to the periplasm, with a small amount present in the cytosol. However, they failed to address the stationary phase dependent synthesis of the enzyme.

In addition to a reduction in growth rate, these investigators also found that DDC increased induction of the superoxide response regulon (soxRS regulon) (Benov and Fridovich 1996). This regulon initiates transcription of a variety of genes of enzymes that scavenge superoxide and repair the damage it causes such as glucose 6-phosphate dehydrogenase, MnSOD, and DNA repair endonuclease IV (Nunoshiba et al. 1992). This may explain why paraquat exerted a greater bacteriostatic effect when used as a single treatment than in combination with DDC. Cells received DDC before paraquat treatment, and it is possible that the cell was already armed with these enzymes before superoxide production by paraquat began. The sharp decline in growth rate observed near the end of the monitoring period may have been due to the depletion of nutrients in the medium resulting in an inability to keep up production of these enzymes and replace damaged proteins.

Assessing cell viability with the LIVE/DEAD BacLight Bacterial Viability Kit

Although the BacLight kit offers a more rapid assessment of cell viability than more traditional methods, it is essential that the kit is calibrated for each bacterial strain. It is interesting that the manufacturer uses a different conversion for optical density measurements to cell number (0.06 OD_{670} = 2 x 10^8 cells/mL) than the standard conversion reported elsewhere in the literature (0.2 OD_{600}= 2 x 10^8 cells/mL). Although the traditional wavelength used for optical density measurements of bacterial cultures is

600 nm, there is nothing specific about this wavelength that would affect cell density measurements since light scattering is being measured and not absorption. Previous experiments using a microplate reader to assess the relationship between the wavelength used for measurement and the resulting growth curve found that a similar curve was obtained at 570, 600, 630, 800, and 850 nm (Quigley 2008). Therefore, it is unlikely that the large difference between OD to cell concentration conversions was a result of the 70 nm difference in wavelength used for measurements.

The high concentrations of dye required for ATCC 4157 when the cell suspension was adjusted to OD_{670} 0.06 were likely caused by a high disproportionality between cell and dye concentrations. As shown in Figure 38, high fluorophore concentrations can prevent light from being transmitted evenly through the sample, with it instead being absorbed completely at the side of the sample facing the light source. By having too few cells and a large excess of dye, fluorescent measurements indicated that higher and higher dye concentrations were needed to saturate the cell suspension. As observed with SYTO9, ultimately the concentration of dye was so high (16 μM) that quenching occurred.

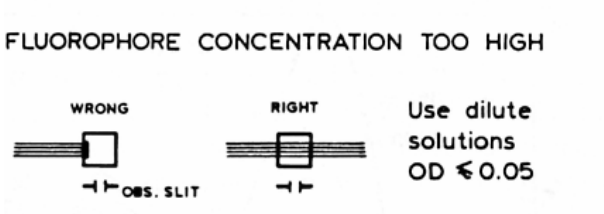

Figure 38. Effect of high fluorophore concentration on light transmittance (from Lakowicz 2006).

However, taking cost and the possibility of the inner filter effect into consideration, choosing dye concentrations that are close to optimal concentrations

should not compromise live/dead discrimination. When determining the concentration of propidium iodide to use, small improvements in the coefficient of determination, for example 0.994 compared to 0.9762 (Figure 28), may not be enough to justify choosing the dye with the higher R^2 value if it is a much higher concentration than the one with the lower R^2 value. Likewise, when evaluating saturation curves for SYTO9, choosing a lower dye concentration could prevent these complications. Often trade-offs must be made between sensitivity and reagent cost as well as available filters.

While the cell concentration was adjusted to 2×10^8 cells/mL based on CFUs/mL vs. OD_{670} data obtained for log phase ATCC 4157, dye calibration for ER2566 was successful using the manufacturer's recommended OD_{670} 0.06 adjustment. This provides further evidence that it is not the concentration of cells that is the most important factor for calibration, but the proportionality between dye and cell concentration. Even though at this OD, calibration data based on both CFU counts and hemacytometer counts indicated that the cell concentration is much lower than that recommended by the manufacturer, clearly saturation concentrations of the dyes were obtained using low dye concentrations.

Generation of extracellular superoxide with the xanthine/xanthine oxidase enzyme system

It is likely, although again speculative, that the differences observed between the effect of X/XO on ER2566 and ATCC 4157 were due to differences between compositions of their outer membranes. Being a known human pathogen, it is probable that ATCC 4157 possesses a greater defense against extracellular oxidative stress than does ER2566. When evaluating the effect of pH on extracellular superoxide-induced cell

death of ER2566, a difference was noted between cell viability at the two pH values tested with CFU counts. While lower CFU counts were obtained for treated cells compared to untreated cells at a pH of 6.5, at a pH of 7.5 CFU counts of treated cells were comparable to those obtained for untreated cells with the exception of the last two measurements. These data support the findings of a previous report that superoxide must be protonated before it can enter the cell (Korshunov and Imlay 2002). However, it is also important to point out that even at a pH of 6.5 these researchers were only able to detect xanthine oxidase-generated superoxide damage using *sodAsodBsodC* mutants and oxygen starved cells. The pH requirement highlights a drawback of the X/XO assay. Within the phagolysosome, protonation of superoxide ($pK_a = 4.8$) is not a problem as the environment is highly acidic (pH 4-5). However, this pH cannot be tested using xanthine oxidase as the enzyme is inactive at low pH.

Comparison between the BacLight kit and spread-plate method for determination of cell viability following X/XO treatment

For ER2566 treated with X/XO-generated superoxide at a pH of 7.5, a greater loss of viability was detected with the BacLight kit than with the spread-plate method. The percentage of cells detected live by the BacLight kit decreased by 24.2% for cells treated with X/XO-generated superoxide, compared to 8% for untreated cells during the treatment period. In contrast, with the spread-plate method, there was not a clear difference between untreated and treated cells until the end of the treatment period. Based on these data, it appears that the BacLight kit offers better discrimination for assessing cell viability.

APPENDIX

Luria-Bertani Broth (LB)
Per Liter

Tryptone	10 g
Yeast extract	5 g
NaCl	5 g
Water to	1 L

Adjust pH to 7.2 with 1 N NaOH

Double Strength Luria-Bertani Broth (2XLB)
Per Liter

Tryptone	20 g
Yeast Extract	10 g
NaCl	10 g
Water to	1 L

Adjust pH to 7.2 with 1 N NaOH

Nutrient Broth (NB)
Per Liter

Peptone	5 g
Beef Extract	3 g
Water to	1 L

Adjust pH to 7.0 with 1 N NaOH

Stab Agar
Per Liter

Tryptone	10 g
Yeast Extract	5 g
NaCl	5 g
Agar	6 g
Cysteine	10 mg
Water to	1 L

Adjust pH to 7.2 with 1 N NaOH

Luria-Bertani Plate Media

Per Liter

Tryptone	10 g
Yeast Extract	5 g
NaCl	5 g
Agar	15 g
Water to	1 L

Adjust pH to 7.2 with 1 N NaOH

1X Phosphate Buffered Saline (PBS)

Per Liter

NaCl	8 g
KCl	0.2 g
Na_2HPO_4	1.44 g
KH_2PO_4	0.24 g
Water to	1 L

Adjust pH to 7.4 with 1 N NaOH

0.85% NaCl

Per liter

NaCl	8.5 g
Water to	1 L

50 mM Potassium Phosphate Buffer (PPB)

KH_2PO_4	3.4
Water to	500 mL

Adjust pH to 7.5 with 1 N KOH

REFERENCES

Benov LT, Fridovich I. 1996. Functional Significance of the Cu,ZnSOD in *Escherichia coli*. Archives of Biochemistry and Biophysics. 327(2): 249-253.

Bus JS, Gibson JE. 1984. Paraquat: Model for Oxidant-Initiated Toxicity. Environmental Health Perspectives. 55: 37-46.

Byrne ST, Gu P, Zhou J, Denkin SM, Chong C, Sullivan D, Liu JO, Zhang Y. 2007. Pyrrolidine Dithiocarbamate and Diethyldithiocarbamate Are Active Against Growing and Nongrowing Persister *Mycobacterium tuberculosis*. Antimicrobial Agents and Chemotherapy. 51(12): 4495-4497.

Carr RJ, Bilton RF, Atkinson T. 1986. Toxicity of Paraquat to Microorganisms. Applied and Environmental Microbiology. 52(5): 1112-1116.

Ehrt S, Schnappinger D. 2009. Mycobacterial Survival Strategies in the Phagosome: Defense Against Host Stresses. Cellular Microbiology. 11(8): 1170-1178.

Fridovich, I. 1995. Superoxide Radical and Superoxide Dismutases. Annual Review of Biochemistry. 64: 97-112.

Harrison R. 2002. Structure and Function of Xanthine Oxidoreductase: Where Are We Now? Free Radical Biology and Medicine. 33(6): 774-797.

Hassan HM, Fridovich I. 1978. Superoxide Radical and the Oxygen Enhancement of the Toxicity of Paraquat in *Escherichia coli*. The Journal of Biological Chemistry. 253(22): 8143-8148.

Heyworth P, Cross A, Curnutte J. 2003. Chronic Granulomatous Disease. Current Opinion in Immunology. 15: 578-584.

Hoerr V, Ziebuhr W, Kozitskaya S, Katzowitsch E, Holzgrabe U. 2007. Laser-Induced Fluorescence-Capillary Electrophoresis and Fluorescence Microplate Reader Measurement: Two Methods to Quantify the Effect of Antibiotics. Analytical Chemistry. 79(19): 7510-7518.

Hopkin K, Papazian M, Steinman H. 1992. Functional Differences Between Manganese and Iron Superoxide Dismutases in *Escherichia coli* K-12. The Journal of Biological Chemistry. 267(34): 24253-24258.

Imlay JA. 2003. Pathways of Oxidative Damage. Annual Review of Microbiology. 57: 395-418.

Imlay JA. 2006. Iron-Sulphur Clusters and the Problem with Oxygen. Molecular Microbiology. 59(4): 1073-1082.

Kao SM, Hassan HM. 1985. Biochemical Characterization of a Paraquat-Tolerant Mutant of *Escherichia coli*. The Journal of Biological Chemistry. 260(19): 10478-10481.

Kargalioglu Y, Imlay JA. 1994. Importance of Anaerobic Superoxide Dismutase Synthesis in Facilitating Outgrowth of *Escherichia coli* upon Entry into an Aerobic Habitat. Journal of Bacteriology. 176(24): 7653-7658.

Karlsson A, Dahlgren C. 2002. Assembly and Activation of the Neutrophil NADPH Oxidase in Granule Membranes. Antioxidants and Redox Signaling. 4(1):49-60.

Kitzler J, Fridovich I. 1986a. The Effects of Paraquat on *Escherichia Coli*: Distinction Between Bacteriostasis and Lethality. Journal of Free Radicals in Biology and Medicine. 2: 245-248.

Kitzler J, Fridovich I. 1986b. Effects of Salts on the Lethality of Paraquat. Journal of Bacteriology. 167(1): 346-349.

Kitzler J, Minakami H, Fridovich I. 1990. Effects of Paraquat on *Escherichia coli*: Differences Between B and K-12 Strains. Journal of Bacteriology. 172(2): 686-690.

Kohanski M, Dwyer D, Hayete B, Lawrence C, Collins J. 2007. A Common Mechanism of Cellular Death Induced by Bactericidal Antibiotics. Cell. 130: 797-810.

Korshunov SS, Imlay JA. 2002. A Potential Role for Periplasmic Superoxide Dismutase in Blocking the Penetration of External Superoxide into the Cytosol of Gram-negative Bacteria. 43(1): 95-106.

Korshunov S, Imlay JA. 2006. Detection and Quantification of Superoxide Formed within the Periplasm of *Escherichia coli*. Journal of Bacteriology. 188(17): 6326-6334.

Lakowicz, J. Principles of Fluorescence Spectroscopy. 3rd ed. New York: Springer, 2006.

McCord J, Fridovich I. 1969. Superoxide Dismutase: An Enzymatic Function for Erythrocuprein (Hemocuprein). The Journal of Biological Chemistry. 244(22): 6049-6055.

Messner K, Imlay JA. 2002. Mechanism of Superoxide and Hydrogen Peroxide Formation by Fumarate Reductase, Succinate Dehydrogenase, and Aspartate Oxidase. The Journal of Biological Chemistry. 277(45): 42563-42571.

Mishell SS, Shiigi SM, eds. Selected Methods in Cellular Immunology. San Francisco: WH Freeman and Co, 1980.

Nunoshiba T, Hidalgo E, Amabile Cuevas CF, Demple B. 1992. Two-Stage Control of an Oxidative Stress Regulon: the *Escherichia coli* SoxR Protein Triggers Redox-Inducible Expression of the soxS Regulatory Gene. Journal of Bacteriology. 174(19): 6054-6060.

Papp-Szabo E, Sutherland C, Josephy PD. 1993. Superoxide Dismutase and the Resistance of *Escherichia coli* to Phagocytic Killing by Human Neutrophils. Infection and Immunity. 61(4): 1442-1446.

Quigley T. 2008. Monitoring the Growth of *E. coli* With Light Scattering Using the Synergy™ 4 Multi-Mode Microplate Reader with Hybrid Technology. Application Note. BioTek Instruments, Inc., Highland Park, Winooski, Vermont.

Raetz CR, Whitfield C. 2002. Lipopolysaccharide Endotoxins. Annual Review of Biochemistry. 71: 635-700.

Stocks SM. 2004. Mechanism and Use of the Commercially Available Viability Stain, *Bac*Light. Cytometry Part A. 61A: 189-195.

Yourassowsky E, der Linden MP, Lismont MJ, Crokaert F, Glupczynski Y. 1985. Correlation between Growth Curve and Killing Curve of *Escherichia coli* after a Brief Exposure to Suprainhibitory Concentrations of Ampicillin and Piperacillin. Antimicrobial Agents and Chemotherapy. 28(6): 756-760.